IL-7 mediated upregulation of VLA-4 increases accumulation of adoptively transferred T lymphocytes in murine glioma.

Authors

1. Kirit Singh, MBBS, MSc[1,2]
2. Kelly M Hotchkiss, PhD[1,2]
3. Sarah L Cook, PhD[1,2]
4. Pamy Noldner, PhD[3]
5. Ying Zhou, BS[3]
6. Eliese M Moelker, BS[1,2]
7. Chelsea O Railton, BS[1,2]
8. Emily E Blandford, BS[1,2]
9. Bhairavy J Puviindran, BS[1,2]
10. Shannon E Wallace, BS, MS[1,2]
11. Pamela K Norberg, BS[1,2]
12. Gary E Archer, PhD[1,2]
13. Beth Shaz, MD[3]
14. John H Sampson MD, PhD, MBA[1,2]
15. Mustafa Khasraw[†]*, MD[1,2]
16. Peter E Fecci*, MD, PhD[1,2,4]

[1]The Preston Robert Tisch Brain Tumor Center at Duke University Medical Center, Durham, NC, US

[2]Department of Neurosurgery, Duke University Medical Center, Durham, NC, US

[3]The Marcus Center for Cellular Cures, Duke University Medical Center, Durham, NC, US.

[4]Duke Center for Brain and Spine Metastasis

[†]Corresponding Author: Mustafa Khasraw, MD

The Preston Robert Tisch Brain Tumor Center

Duke University | Box 3624, Durham, NC 27710

T +1 919.684.6173 | F +1 919.681.1697

mustafa.khasraw@duke.edu

*These authors contributed equally to the manuscript.

Keywords

Immunotherapy; T cells; Cell migration/adhesion

Conflict-of-interest statement

1. KS reports no relevant disclosures.
2. KMH reports no relevant disclosures.
3. SLC reports grants paid to her institution from Immorna Therapeutics, Immvira Therapeutics.
4. PN reports no relevant disclosures.
5. YZ reports no relevant disclosures.
6. EMM reports no relevant disclosures.
7. COR reports no relevant disclosures.
8. EEB reports no relevant disclosures.
9. BP reports no relevant disclosures.
10. SW reports no relevant disclosures.
11. PKN reports no relevant disclosures.
12. GEA reports no relevant disclosures.
13. BS reports no relevant disclosures.
14. JHS reports an equity interest in Istari Oncology, which has licensed intellectual property from Duke related to the use of poliovirus and D2C7 in the treatment of glioblastoma. JHS is an inventor on patents related to Brain Bi-specific T cell Engagers (BRiTE), PEP-CMV DC vaccine with tetanus, as well as poliovirus vaccine and D2C7 in the treatment of glioblastoma.
15. MK reports consultant or advisory roles for Janssen, and Jackson Laboratory for Genomic Medicine; research funding from Daiichi Sankyo, Immorna Therapeutics, AbbVie, Bristol-Myers Squibb.
16. PEF reports no relevant disclosures.

Author contribution: Design, acquisition, analysis of data, and writing of manuscript: KS with assistance from KMH, SLC, PN, YZ, EM, COR, EEB, BJP, SEW, PKN, GEA, BS, JHS, MK and PEF. Overall supervision throughout by JHS, MK and PEF.

Manuscript Details

Abstract Word Count: 200

Body Text Word Count: 6888

Figures: 6 (Supplemental: 3)

Tables: 1 (Supplemental: 1)

Graphical Abstract

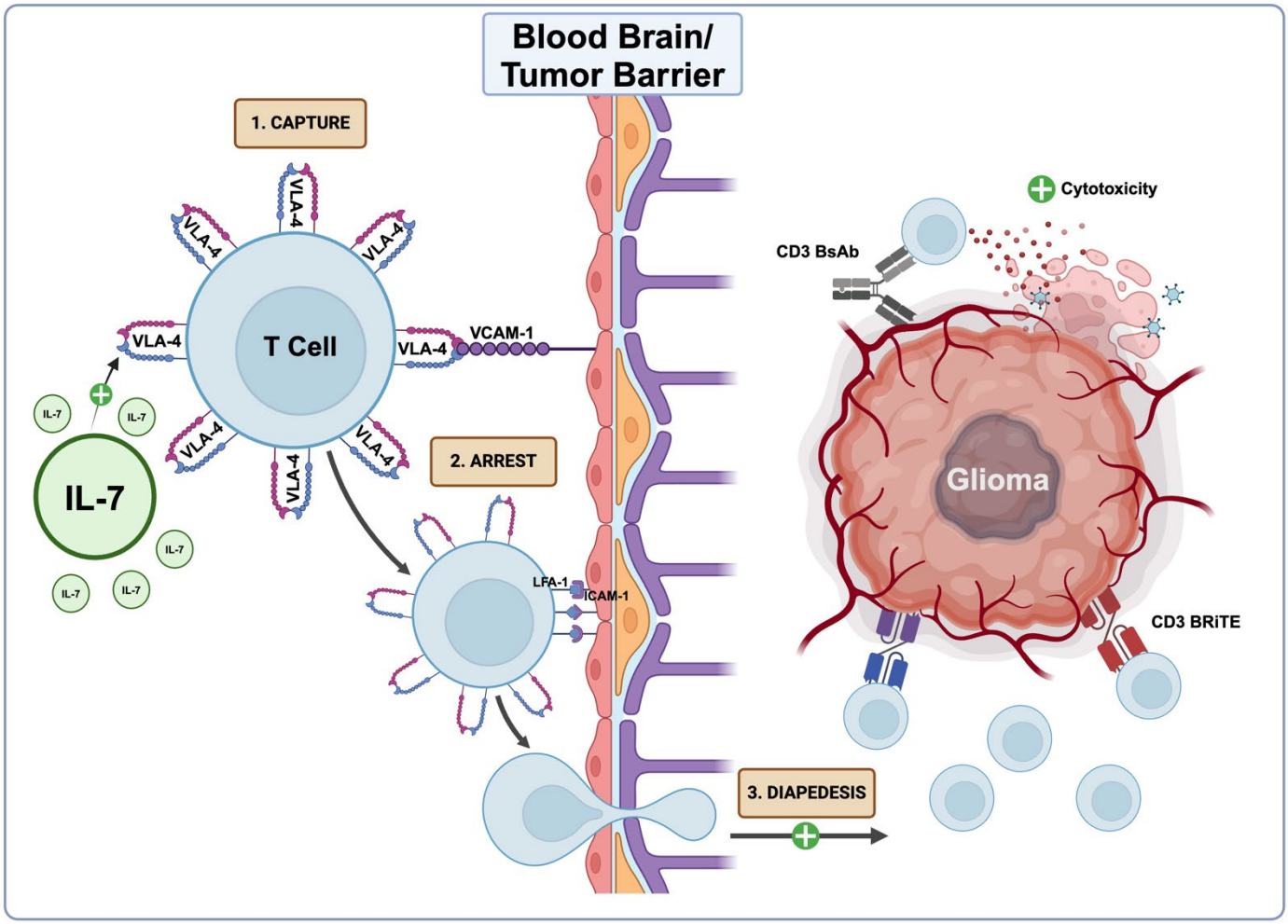

Abstract

The efficacy of T cell-dependent immunotherapies against glioma is limited by few intra-tumoral lymphocytes and tumor-induced T cell sequestration. We considered whether peripheral autologous lymphocyte transfer (ALT) could boost Central Nervous System (CNS) T cell counts in established glioma. We found that ALT lymphocytes specifically entered tumor tissue while endogenous T cell counts fell. T cells expanded with IL-7 demonstrated an enhanced ability to accumulate in established murine glioma compared to IL-2. Increased entry was not phenotype dependent. Instead, IL-7 upregulates the migratory integrin VLA-4 on mouse and human T cells. VLA-4 expression was also high on endogenous T cells in established tumors. Intracranial (IC) VLA-4 blockade retained T cells in the brain but did not yield any survival benefit. IC VLA-4 blockade also reduced the cytotoxicity of immunotherapies *in vitro*. However, combination IL-7 ALT (VLA-4^{Hi}) & α4-1BB antibody therapy extended median survival for animals with orthotopic glioma compared to monotherapy. Similarly, IL-7 expanded hPBMCs & brain bi-specific T cell engagers targeting EGFRvIII (BRiTE) extended survival. We conclude that IL-7 upregulates VLA-4 on T cells, facilitating their accumulation in IC glioma. Seeding gliomas with infiltrative T cells is a potential therapeutic strategy to enhance the efficacy of T-cell dependent therapies.

Brief Summary

T cell immunotherapies are limited by low T cell counts in glioma. IL-7 increases T cells infiltration into tumors, enhancing the efficacy of said immunotherapies.

Introduction

T cell-dependent cancer immunotherapies, such as brain bi-specific T cell engagers (BRiTE) or immune checkpoint blockade (ICB), require the presence of functional T cells at the tumor to be effective[1-3]. This is a hurdle for many solid tumors where low activated T cell counts are seen. Unfortunately, tumors of the central nervous system (CNS) have additional limitations to T cell trafficking and drug localization. CNS tumors exist in an immunologically distinct environment shielded by the blood-brain barrier (BBB) and possess the unique ability to sequester naïve T cells in bone marrow[4]. High-grade gliomas are accordingly known to possess low numbers of Tumor Infiltrating Lymphocytes[5] (TIL) and have proven unresponsive to ICB in clinical trials[6-8]. In addition to low numbers, the paucity of these TILs will likely limit the therapeutic efficacy of newer synthetic therapies that rely on an endogenous T cell response, such as BRiTEs[9].

To overcome this limitation, new therapeutic strategies are required that increase the presence of functional lymphocytes within the IC compartment. These require either the expansion of the local population, increased trafficking from the periphery, or the addition of lymphocytes from elsewhere. However, such strategies face significant challenges. Expansion of the local population is limited by the severe exhaustion of resident $CD8^+$ T cells which makes them non-responsive to stimulation[10] and incapable of cytotoxic activity. Lymphocyte activity and recruitment can be boosted by the use of immunostimulatory cytokines such as IL-12[11] but peripheral administration can result in significant systemic toxicity[12,13]. These barriers may be overcome via local administration, but this requires an invasive procedure which may limit the potential for repeated administrations[14,15].

Peripherally infused CAR-T cells have been shown to cross the BBB and infiltrate into the tumors of patients with glioblastoma[16]. However, the presence of peripherally administered CAR-T cells in tumors has only been detected in tissue collected shortly after administration, indicative of their limited persistence[16]. Modalities that permit repeated delivery and can sustain T cell populations in tumor are therefore desirable. Peripheral Autologous Lymphocyte Transfer (ALT) of an optimized population is one potential approach. Administration of ALT with pro-infiltrative characteristics could seed tumors with a functional TIL population prior to cycles of antibody therapy.

Traditionally, cellular therapies have used Interleukin-2 (IL-2) for *ex vivo* expansion. However, expansion with IL-2 drives T cells towards a terminal effector phenotype[17] resulting in a short lifespan once removed from co-culture. The only alternative growth factor that can independently support T cell expansion is Interleukin-7 (IL-7)[18]. IL-7 is a key mediator of T cell homeostasis[19] and drives T cells towards a memory phenotype in the periphery[20]. Further, IL-7 has been shown to enhance the ability of CAR-T cells to infiltrate into solid tumors[21] and peripheral administration of IL-7 has been demonstrated to increase the presence of effector $CD8^+$ T cells in murine glioma models[22]. We therefore sought to evaluate whether expansion with IL-7 would yield a cellular product with favorable BBB-penetrance and enhanced anti-tumor efficacy in the context of established intracranial glioma.

Herein, we demonstrate that exogenous IL-7-mediated upregulation of Very Late Antigen-4 (VLA-4) enhances peripheral T cell entry into IC tumor tissue, while antibody blockade of the VLA-4 / Vascular Cell Adhesion Molecule-1 (VCAM-1) axis retains T cells in the CNS of mice with established glioma. Further, we establish that IL-7 upregulates VLA-4 expression on

human peripheral blood mononuclear cells (PBMCs) from both healthy volunteers and patients with glioblastoma, permitting clinical translation of our findings.

Results

IL-7-expanded autologous T cells demonstrate enhanced accumulation within orthotopic glioblastoma models despite endogenous T cell sequestration in bone marrow.

Although the transit of peripherally administered autologous T cells across the BBB has been observed under normal physiological conditions[23], their ability to enter and persist in the CNS in the face of tumor-imposed T cell sequestration was unclear. Previous work by our group has established that sequestration predominantly impacts naïve endogenous or adoptively transferred T cells, while memory T cells remained largely undisturbed[4]. We therefore set out to determine whether *ex vivo* expanded non-naïve autologous T cells might retain the capacity to enter and accumulate within CNS tumors.

We first developed T cell expansion processes designed to preferentially expand effector ($T_{EFF,}$ $CD44^{high}CD62L^{low}$) or central memory ($T_{CM,}$ $CD44^{high}CD62L^{high}$) subsets. Expansion of T cells with either 100IU/mL IL-2 or 20ng/mL IL-7 supplementation skewed our cellular product to enrich for $CD8^+$ T_{EFF} or $CD8^+$ T_{CM} phenotypes respectively[18,24,25]. At the end of the expansion process, we performed flow cytometry analysis to assess phenotypic ratios (**Figs. S1A, S1B**). *Ex vivo* expansions with both IL-2 and IL-7 produced a cellular product that consisted of >95% $CD3^+$ cells (**Fig. S1C**). For both IL-2- and IL-7-expansions, the product predominantly consisted of $CD8^+$ cells (~80%) (**Fig. S1D**). As expected, IL-2-expansion was preferentially selected for a T_{EFF} population (**Fig. S1E**) while IL-7 expanded the T_{CM} population (**Fig. S1F**). Low proportions of naïve $CD8^+$ T cells (T_N, $CD44^{low}CD62L^{high}$) populations were identified in both products at the end of expansion (**Fig. S1G**).

To establish the trafficking capabilities of T cells exposed to these different conditions, we implanted CT-2A stably transfected with EGFRvIII (CT2AvIII), into $CD45.2^+$ mice. After tumors had become established for 13 days, mice were administered either IL-2 or IL-7-expanded $CD45.1^+$ T cells (**Fig. 1A**). Exogenous and endogenous $CD3^+$ populations were analyzed over the ensuing 4 days in both brain and bone marrow. This period reflects a typical window in which T cell sequestration is observed, as this model approaches survival endpoint[4]. Regarding tumor, examination of the exogenously administered $CD8^+$ populations revealed that these cells accumulated over time, peaking at approximately 72 hours following administration**.** We observed that IL-7-expanded ALT accumulated at a higher rate within tumor hemispheres compared to IL-2 ALT **(Fig. 1B, C,** 72-hours IL-7 median 26.66x vs IL-2 median 4.291x, p=0.0159***)**. Interestingly, while IL-7 ALT accumulated within tumor after administration, endogenous T cell numbers declined within tumor over the same period. Simultaneously we observed increases in bone marrow $CD3^+$ T cell counts over time across all groups (**Fig. 1D**). Endogenous T cells and exogenously administered ALT populations did not differ in their relative accumulation within bone marrow **(Fig. 1E,** 72-hours endogenous median fold-increase 1.73x vs IL-7 median fold-increase 1.92x, p=0.2381**)**. Additionally, while spleen sizes diminished in all tumor-bearing mice (as seen previously[4]), we noted a transient increase in spleen sizes following ALT, before resumption of decline (**Fig. 1F**).

We then examined whether IL-2 or IL-7 ALT would result in enhanced survival when combined with antibody-based T cell-dependent immunotherapies. First, we combined each ALT with EGFRvIII-BRiTE in a U87 xenograft model which has been stably transfected to express EGFRvIII (U87vIII). EGFRvIII-BRiTE is a bi-specific T cell engager that tethers the CD3 receptor to the glioma specific antigen EGFRvIII[26]. As EGFRvIII-BRiTE is a fully human construct, we evaluated this in an NSG model that was reconstituted with either IL-7 or IL-2-expanded human (h)PBMCs. We observed that IL-7 expanded ALT yielded a significant survival benefit when combined with BRiTE compared to the IL-2 ALT (**Fig. 1G**, p=0.0496*), despite a similar *in vitro* cytotoxicity (**Fig. S1H**). We also evaluated both ALT conditions in an immunocompetent setting, using C57Bl/6 mice and different antibody-based therapies to determine which combinations might be most effective. After CT2AvIII tumors were allowed to establish for 10 days, animals were treated with either IL-7 ALT alone, or combinatorial therapy with αCTLA-4, αPD-1 or α4-1BB monoclonal antibodies (**Fig. S1I**). We found that the combination of IL-7 and α4-1BB yielded the greatest survival benefit compared to ALT monotherapy at end of follow-up (**Fig. S1J**, p=0.0134*). Based on these findings, we selected this combination approach for further experiments, and performed survival studies with appropriate controls using the same study design as before (initiation of therapy on IC Day +10, **Fig. 1H**). We again found that IL-7 ALT & α4-1BB therapy yielded the greatest survival benefit, with significant increases in efficacy compared to combination IL-2 ALT & α4-1BB (p=0.0132*).

Increased accumulation of IL-7 expanded CD8$^+$ lymphocytes in tumor consists of both central and effector memory phenotypes.

Having observed the superior trafficking characteristics and anti-tumor efficacy of IL-7 ALT, we wanted to determine whether this was attributed to the increased central memory population or global changes in migratory integrins. Frequent antigenic stimulation can upregulate the expression of trafficking molecules on T_{CM} cells, facilitating their ability to cross endothelial barriers[27,28]. However, T_{EFF} cells also upregulate migratory ligands such as LFA-1 and VLA-4 involved in binding to endothelial surfaces following activation[29,30]. We therefore first sought to evaluate the phenotypic makeup of exogenous T cells that had entered the brain following ALT, looking to distinguish CD8$^+$ T_{EFF} or T_{CM} populations before subsequent evaluation of migratory integrin expression.

To begin, C57Bl/6 CD45.2$^+$ mice were implanted with the same IC CT-2AvIII line. Given we had observed sustained efflux of endogenous T cell dynamics from tumor at D15-D17 in our prior experiment, tumors were allowed to establish for 15 days for follow-up. Mice were then intravenously administered autologous CD45.1$^+$ T cells that had been expanded with either IL-2 or IL-7. At 3-hours and 48-hours following administration, tumors were harvested and analyzed for T cell accumulation and phenotype by flow cytometry (**Fig. 2A**). We again observed significantly enhanced tumor accumulation of IL-7 ALT at both 3- (p=0.0022**) and 48- (p=0.0159*) hours following administration compared to IL-2 ALT (**Fig. 2B**). Phenotyping of administered T cells in the CNS 48-hours following ALT showed that for both expansion conditions, >95% were CD8$^+$ lymphocytes (**Fig. 2C**). By 48-hours post administration, CD45.1$^+$ IL-7 ALT cells made up approximately 20% of the total CD3$^+$ population in tumor tissue (exogenous and endogenous combined) (**Fig. 2D**, mean 19.4%, SD ±4.53%, n=5), while the percentage of IL-2 ALT was negligible. Subset analysis revealed that for IL-7 ALT, the proportions of CD8$^+$ T_{CM} and T_{EFF} accumulating in tumor were similar (46.5% and 42.5%, respectively, **Fig. 2E**). IL-2 ALT phenotypes mirrored those of endogenous T cells accumulating in tumor and were predominantly T_{EFF} (IL-2 ALT in tumor: CD8$^+$ T_{CM} 14.5% and CD8$^+$ T_{EFF}

83.2%, endogenous in tumor: CD8$^+$ T_{CM} 17.6% and CD8$^+$ T_{EFF} 68.8% **Fig. 2F**). Despite this, the absolute counts per gram of IL-7-expanded CD8$^+$ T_{EFF} cells found in tumor was greater than the numbers of IL-2 CD8$^+$ T_{EFF} (**Fig. 2G**, p=0.0159*, CD8$^+$ T_{CM} shown in **Fig. 2H**, p=0.0159*). We could therefore surmise that differential entry characteristics were not just a CD8$^+$ T_{CM} phenomenon but were occurring across both CD8$^+$ T_{CM} and T_{EFF} subsets.

Expansion with IL-7 upregulates expression of the pro-migratory integrin VLA-4 on murine CD8$^+$ cells, which is necessary for enhanced intra-tumoral accumulation.

Given the phenotype-independent differences in intratumoral accumulation between IL-7 ALT and IL-2 ALT, we subsequently analyzed the expression of integrins involved in migration into tissues (VLA-4, LFA-1) on exogenous T cells that entered the CNS following administration. We observed that expression of VLA-4 was significantly increased on IL-7 ALT cells at the 3-hour (**Fig. 3A**, p=0.0173*) and 48-hour (**Fig. 3B,** p=0.0079**) timepoints compared to on IL-2 ALT, whereas LFA-1 expression on ALT in tumor was not significantly different between the two expansion conditions (**Fig. 3C**, p=0.1775). This was also true prior to administration of the cellular product (**Fig. 3D**, representative VLA-4 gating shown in **Fig. 3E**, LFA-1 gating in **S2A**), in which the greatest change in VLA-4 expression was observed on the T_{EFF} subset. This aligned with our analysis of VLA-4 expression on phenotypic subsets in tumor where VLA-4 was most increased on the T_{EFF} subset, although this difference was not significant compared to either the T_{CM} or T_N subsets (**Fig. S2B**, CD8$^+$ T_{EFF} vs T_{CM}, p=0.6991, CD8$^+$ T_{EFF} vs T_N, p=0.1797).

To evaluate the impact of VLA-4 on trafficking, we began by selecting cultured T cells that were VLA-4^{Hi} or VLA-4^{Lo} using flow cytometry (Geometric MFI (gMFI) shown in **Fig. S2C,** VLA-4^{Hi} average gMFI 1603, SD ±374.3, n=4 vs VLA-4^{Lo} average gMFI 683, SD ±105, n=2). These two populations were then administered to animals with 15-day established tumors. The VLA-4 blocking antibody, natalizumab[31], was also administered as a single dose (200 µg) intraperitoneally prior to ALT in a sub-group. We hypothesized that the addition of VLA-4 blockade to VLA-4^{Hi} ALT would reduce T cell entry to levels seen with our VLA-4^{Lo} ALT group. 48 hours following administration, tumors were harvested and analyzed for entry of exogenous T cells into the CNS. Pooled analyses demonstrated that increased entry of CD45.1$^+$CD8$^+$ VLA-4^{Hi} T cells into tumor was abrogated by natalizumab (**Fig. 3F**, VLA-4^{Hi} vs VLA-4^{Lo}, p=0.0491*; VLA-4^{Hi} vs αVLA-4 & VLA-4^{Hi}, p=0.0428*). Counts were similar for VLA-4^{Lo} and αVLA-4 & VLA-4^{Hi} (p=0.9626).

We also evaluated the effect of adding natalizumab to our combination therapy of IL-7 ALT and α4-1BB. We found that IL-7 ALT & α4-1BB therapy yielded the greatest survival benefit (median survival 54 days), compared to monotherapy with α4-1BB only (median survival 37 days) or IL-7 ALT alone (median survival 24 days). Administration of intraperitoneal natalizumab (αVLA-4, 200µg) 1 hour prior to ALT abrogated the enhanced survival benefit, and median survival (30 days) fell to below that obtained with α4-1BB monotherapy (**Fig. 3G**). We therefore concluded that IL-7 upregulated VLA-4 on murine CD8$^+$ cells in culture and that this enhanced trafficking into tumor hemispheres was dependent on the VLA-4/VCAM-1 axis.

VLA-4 expression is increased on endogenous T cells in tumor.

While examining the degree of VLA-4 expression on ALT, we also noted that VLA-4 expression was even higher on the endogenous $CD8^+$ lymphocytes found in tumor (**Fig. 4A**, VLA-4 gMFI of endogenous $CD8^+$ compared to ALT $CD8^+$ cells in tumor, p=0.0039*), with expression increasing from day 15 to day 17 following tumor implantation (**Fig. 4B**). To determine whether the increased VLA-4 expression seen on endogenous IC T cells was a phenomenon specific to brain tumor infiltrates, we first analyzed the makeup of the various tissue compartments in mice bearing IC CT-2AvIII tumors. Animals did not receive ALT so we could observe patterns of VLA-4 expression without an exogenous influence. Mice were sacrificed on Day 16 following tumor implantation and brain, spleen, bone marrow, lungs, and blood collected (**Fig. 4C**).

When evaluating VLA-4^{Neg}, VLA-4^{Mid} and VLA-4^{Hi} fractions across all compartments, we again observed a larger VLA-4^{Hi} population in brain tumor compared to all other tested compartments (**Fig. 4D** mean fraction in brain 19.88%, SD ± 6.27%). We also found that the largest endogenous subset present in murine glioma is $CD8^+$ T_{EFF} cells (**Fig. 4E**, mean fraction 59.36%, SD ± 13.28%), and that VLA-4 gMFI is equally increased across $CD8^+$ T_{EFF} and T_{CM} subsets (**Fig. 4F,** $CD8^+$ T_{EFF} vs T_{CM} p=0.6905). We therefore considered whether intracranial blockade of VLA-4 might prevent T cells from exiting the CNS, thereby increasing their intratumoral accumulation .

Intracranial VLA-4 blockade enhances intratumoral T cell accumulation but does not enhance survival and reduces the cytotoxicity of immunotherapies dependent on immune synapse formation.

We began by comparing the effect of intraperitoneal (IP) vs intra-tumoral administration of natalizumab on the accumulation of T cells in mice with IC CT-2AvIII. Sham IC injections of phosphate buffered saline (PBS) were used as a control for immune recruitment following surgery (**Fig. 5A**). Tumors were harvested 24- and 72 hours following administration to evaluate changes in T cell numbers and VLA-4 expression. Spleens were also analyzed at the same time points to observe changes to a peripheral compartment. Pharmacokinetic analyses from clinical and *in vitro* studies have found that free natalizumab levels are 100-fold reduced in cerebro-spinal fluid (CSF) compared to serum concentrations[32]. As a result, we selected dose levels of 200 µg natalizumab IP and 2 µg IC.

At these doses, we observed that intratumoral $CD4^+$ and $CD8^+$ T cell populations were unchanged at 24-hours, but both significantly increased 72-hours following IC administration of natalizumab compared to sham IC (72-hr $CD4^+$ IC aVLA-4 vs sham p=0.0317*, 72-hr $CD8^+$ IC aVLA-4 vs sham p=0.0317*), whereas IP administration reduced intratumoral counts of both (**Figs. 5B-E**). IC VLA-4^{Hi} fractions fell 24-hours following IC administration of αVLA-4, but this decrease was transient, and the VLA-4^{Hi} fraction increased again 72-hours following IC administration (**Fig 5F**). IP αVLA-4 resulted in sustained suppression of VLA-4 on $CD8^+$ cells throughout (**Fig. 5G**). In the spleen, we observed a decline in VLA-4 levels on $CD4^+$ and $CD8^+$ T cells with IP natalizumab. Interestingly, there was also a small and transient decrease in VLA-4 levels following IC natalizumab, perhaps suggesting antibody escape from the CNS, although VLA-4 levels returned to normal by 72-hours post administration (all treatments: splenic $CD4^+$ shown in **Fig. S3A** and splenic $CD8^+$ shown in **Fig. S3B**).

Having established that IC VLA-4 blockade increased T cell counts in IC tumors, we next wanted to determine the therapeutic implications. We first evaluated direct IC VLA-4 blockade as a monotherapy or combined with α4-1BB where we had observed synergism with IL-7 ALT previously. Mice with 10-day established CT2AvIII tumors were treated IC with 2 μg natalizumab and IP α4-1BB (4 treatments of 200 μg every 3 days from D10 to D19). Despite the observed increase to intratumoral endogenous T cell numbers, no survival benefit was seen when treating with IC αVLA-4 monotherapy or combination IC αVLA-4 and IP α4-1BB (**Fig. 5H**). As VLA-4 forms a key part of the activation complex of the immune synapse[33], we considered whether VLA-4 blockade might reduce T cell cytotoxicity when combined with CD3-engaging therapies like BRiTE.

To determine this, we performed *in vitro* co-culture cytotoxicity assays using CT2AvIII and BRiTE. We established concentrations of BRiTE that either resulted in no kill, 50% kill (half-maximal effective concentration, EC_{50}) or near total kill (**Fig. S3C**) when co-culturing with T cells and tumor cells. We predicted that any blunting of BRiTE's anti-tumor effect would be most apparent at the EC_{50} concentration. We found that αVLA-4 *in vitro* did not possess any direct anti-tumor cytotoxic effect (**Fig. 5I**) but did decrease cytotoxicity when BRiTE was included at the established EC_{50} concentration of 0.01 μg/mL from 48.45% to 20.37% (**Fig. 5J**, $p<0.0001$****). Based on these findings, we surmised that VLA-4 blockade may interfere with T cell cytotoxicity.

We concluded that seeding tumors with highly infiltrative T cells via ALT would reflect the optimal approach for combination with T cell dependent therapies. Thus, for translation to the clinic, we wanted to determine whether a) whether leukapheresis products from patients with glioblastoma would respond / expand in the same manner as healthy controls, and b) similar skewing of the VLA-4 axis occurred when expanding human T cells with IL-7.

IL-7 expansion of hPBMCs from both healthy volunteers and patients with glioblastoma enhances lymphocytic VLA-4 expression.

We first sought to establish whether our expansion processes could be applied to frozen leukapheresis products taken from both healthy control volunteers and patients with glioblastoma. Samples were used from healthy volunteers (collected under institutional donor protocol, Duke IRB: #Pro00009403) and compared with historical leukaphereses from glioblastoma patients who had enrolled on clinical trials and consented to *ex vivo* expansion of PBMCs for research purposes (**EXCEL:** Newly diagnosed GBM patients prior to RT and TMZ, $EGFRvIII^+$ Tumors, NCT02664363, Duke IRB #Pro00069444) & **INTERCEPT:** Recurrent GBM patients, $EGFRvIII^+$ Tumors, NCT03283631, Duke IRB #Pro00083828). An overview of donor demographics and pathology is shown in **Table 1**. Median ages between groups were similar (controls median age 54.3yo vs patient median 58.7yo) with a 2:1 M:F ratio in both groups. Of the glioblastoma samples, 5 of 6 were collected from patients receiving dexamethasone.

Samples from control and glioblastoma groups were thawed and activated with αCD3/αCD8 nanoparticles. Cultures were maintained for 14 days in media supplemented with 300IU/mL IL-2 as per our CAR-T expansion protocols (without transduction)[34] or 20ng/mL IL-7. At the end of the expansion process, cell counts, phenotyping and assessment of activation as well as VLA-4 expression was evaluated (**Figs. S4A, S4B**).

While both expansion conditions were capable of independently supporting T cell growth (**Fig. 6A**), IL-2 produced greater yields – over 2 fold higher expansion - for both volunteer control and GBM samples (**Fig. S4C**, p=0.0043**). There was no significant difference between volunteer and glioblastoma T cell expansion rates when co-cultured with either IL-2 or IL-7. Final expansion product consisted of ~95% $CD3^+$ across all samples and conditions (**Fig. S4D**). However, we did observe that IL-7 expansion skewed significantly more towards $CD4^+$ (~60:40 ratio of $CD4^+$:$CD8^+$) whereas IL-2 skewed towards $CD8^+$ ($CD4^+$:$CD8^+$ ~ 33:66, **Figs. 6B**, **6C**), which differed from our mouse expansion findings (~80% $CD8^+$ for IL-2 and IL-7). It is unclear whether this was due to differential responses to IL-7, or different stimulatory products used for expansion.

On deep phenotyping of memory and effector subsets, we observed that T_{EFF} ($CD45RO^-CD45RA^+CD95^+CCR7^-$) and T Effector Memory (T_{EM}, $CD45RO^+CD45RA^-CD62L^-CCR7^-$) fractions were similar between IL-2 and IL-7 expansion groups (T_{EFF} in **Fig. S4E**, T_{EM} fractions in **Fig. S4F**, all subsets shown in **Fig. 6D**). However, IL-7 did promote the expansion of the stem cell memory subset (T_{SCM}, $CD45RO^-CD45RA^+CD95^+CCR7^+$). IL-7 is known to preferentially expand T_{SCM} subsets[35] and this subset has been suggested to have greater antitumor potential due to their self-renewing capabilities[36]. Aligning with this, we observed that IL-7 expansion of both control and glioblastoma hPBMCs increased the T_{SCM} fraction, but only glioblastoma samples yielded a significant increase compared to IL-2 (**Fig. 6E**, p=0.0313*).

We then sought to evaluate whether our IL-7 increased VLA-4 expression on human T cells, as we found with our mouse model. Given we anticipate this as an adoptive cellular therapy to combine with cytotoxic T cell re-directing treatments, we focused on the $CD8^+$ population. We evaluated VLA-4 expression and classed cells as VLA-4^{Neg}, VLA-4^{Mid} or VLA-4^{Hi} by flow cytometry (**Fig. 6F**). For both control and glioblastoma samples, IL-7 expansion significantly increased the VLA-4^{Hi} fraction over that seen with IL-2 (**Fig. 6G**, GBM IL-2 $CD8^+$VLA-4^{Hi} vs GBM IL-7 $CD8^+$VLA-4^{Hi}: 34.1% vs 86.9%, p=0.0087**, $CD8^+$ gMFI shown in **Fig. S4G**). We only observed significant VLA-4 increases on $CD8^+$ T_{EFF} and $CD8^+$ T_{SCM} subsets (**Figs. 6H, 6I**, p=0.0022**), while changes on $CD8^+$ T_{EM} were not significant (**Fig. S4H**, p=0.1797). Similar dynamics were observed on the $CD4^+$ population, with significantly increased VLA-4 gMFI when culturing with IL-7 (**Fig. S4I,** GBM IL-2 vs GBM IL-7, $CD4^+$ VLA-4 gMFI: 2477 vs 4886, p=0.0022**), Finally, we performed a parallel cytotoxicity assay comparing expanded volunteer T cells and glioblastoma patient T cells. To determine *in vitro* potency, we used BRiTE and U87vIII *in vitro* as per prior experiments and found similar cytotoxicity profiles between controls and glioblastoma samples (**Fig. 6J**).

Discussion

Bispecific T cell-engagers are antibody fragments designed to bring T cells close to target cells and activate them for efficient killing. Their potential specificity, potent activation, bystander killing, and reduced immunogenicity make them a promising strategy for cancer immunotherapy[37]. However, for this approach to be effective against tumors of the CNS, they must be able to encounter immune cells within the IC compartment. Although immune cells can cross the BBB[23], primary CNS malignancies are surrounded by a highly immunosuppressive TME[38] and likewise are capable of “driving” T cells away, sequestering them in the bone marrow[4,39].

Our results demonstrate that adoptively transferred expanded T cells can specifically enter tumor tissue despite endogenous T cell sequestration and can do so in sufficient quantities to augment T cell-dependent therapies such as BRiTE or α4-1BB. We observed that IL-7 expanded T cells demonstrated an enhanced capacity to enter the CNS, resulting in greater intra-

tumoral T cell density. Campian *et al* recently found that peripheral administration of long-acting recombinant IL-7 enhanced numbers of cytotoxic $CD8^+$ T lymphocytes systemically and in tumor for similar animal models of glioma[22]. Our study expands upon these results, finding that IL-7 both supports lymphocyte expansion and enhances expression of the migratory integrin VLA-4 across $CD8^+$ subsets. IL-7's effect on upregulating VLA-4 has been previously reported *in vitro*[40], and peripheral administration of recombinant human IL-7 (rhIL-7) has been observed to increase VLA-4 and T cell trafficking in murine models of sepsis[41]. Similarly, tumor-mediated downregulation of VLA-4 via IL-4 and the Jak-Stat6 pathway has been found to prevent the infiltration of T cells into IC malignancies[42]. Our findings therefore align with these prior studies and extrapolate this mechanism to the adoptive cellular therapy context for IC malignancies.

While we observed that IL-2 produced greater yields and $CD8^+$ skewing than IL-7 in hPBMC samples, we noted that IL-7 significantly increased the $CD8^+$ T_{SCM} fraction and enhanced VLA-4 expression specifically on $CD8^+$ T_{EFF} and CD8+ T_{SCM} subsets. We can therefore envisage a culturing process that yields significant quantities of effector and stem-like memory populations and upregulates VLA-4. Before administration to patients, selection based on VLA-4 expression could be undertaken to choose highly infiltrative cells. Given that the VLA-4/VCAM-1 migratory axis is tumor histology-agnostic, this approach could be used to inflame not just primary malignancies but also for the treatment of immunologically cold metastatic disease[43]. Importantly, IL-7 cellular expansion is already in the clinic and has been used to support CAR-T expansion in clinical trials[44]. Although the use of IL-7 has been used to mediate superior longevity and engraftment due to its homeostatic function[45], our findings would suggest that IL-7 also facilitates the entry of T cells into the CNS.

Notably, our study finds closely aligned patterns of behavior between both volunteer and patient leukapheresis in terms of expansion rates, phenotypic skewing, VLA-4 expression, and *in vitro* cytotoxicity. The evidence base comparing expansion characteristics of leukapheresis from patients with GBM and healthy donors is limited, and much pre-clinical work often uses healthy donor samples from commercial sources. However, glioblastoma can induce profound changes in T cell function[46] and previous reports have described that T cells from patients with primary IC tumors can exhibit impaired activation responses[47]. Our study therefore provides a controlled and contemporaneous evaluation of these dynamics using samples from the clinic and indicates that findings in healthy donor samples will translate to the pathological setting, even when patients are receiving steroid therapy. We observed that T cells from patients with glioblastoma retain the same potential for growth, activation, phenotypic skewing, and *in vitro* cytotoxicity as healthy volunteers when removed from the host and expanded in culture.

To our knowledge, this is the first time that increased VLA-4 expression on endogenous $CD8^+$ lymphocytes in CNS tumors has been described. While VLA-4 blockade did effectively retain T cells inside the CNS, it failed to induce any significant survival benefit as monotherapy or when combined with α4-1BB. Further, we observed that VLA-4 blockade may blunt the efficacy of immunotherapies, such as BRiTE, that are reliant on forming an immunological synapse with tumor. Nevertheless, our observation that VLA-4 levels increased on T cells even in the context of tumor-imposed T cell sequestration may reflect a future therapeutic axis. While we did not fully delineate the underlying mechanism, VLA-4 upregulation and memory T cell accumulation in the context of glioma has been described following repeated antigenic exposure and stimulation when administering dendritic cell vaccines pulsed with tumor lysate[48]. Sustained antigen exposure in the context of a heterogenous tumor could progressively increase migratory integrins and contribute to T cell efflux from the CNS. Further exploration of targeting this axis to retain T cells at the tumor site may therefore be warranted. IC blockade

of the VCAM-1 receptor may achieve desired retention of T cells in tumor while avoiding interfering with immune synapse formation.

For this study, we elected to evaluate both IL-2 and IL-7, as we had previously established that they could independently support T cell expansion[18]. Similarly, we used doses of IL-2 and IL-7 that had been established previously to expand T cells in both mice and humans. However, cytokines such as IL-15, IL-18, IL-21 and others have been used in varying concentrations to supplement the expansion process[49]. We also appreciated that the IL-7 receptor is downregulated after sustained exposure and it may be that intermittent cycling with IL-7 is the preferential approach[50]. Our study is therefore limited to assessing the dynamics of these two cytokines at this single dose level. However, given the wide array of potential permutations, identifying the optimal combination, dose, and schedule for cytokine expansion of autologous T cells will require a sustained process development approach. We also evaluated trafficking dynamics in a single mouse model of glioma, and although similar models have been used to demonstrate sequestration previously[4], it is possible that T cell behavior could vary between models.

In conclusion, we find that IL-7 expansion of autologous T lymphocytes upregulates VLA-4 on these cells and enhances their ability to accumulate in IC murine glioma. Intra-cranial blockade of VLA-4 retains T cells in tumor but can have negative effects on T cell cytotoxicity. Our study includes observations in both murine and human settings, with similar changes in integrin expression occurring for hPBMCs from both healthy volunteers and patients with glioblastoma. Future development of T cell expansion processes for IC malignancies should consider selecting $CD8^+$ cells with high VLA-4 expression if intending to peripherally administer autologous cells. The findings of this study will be used to inform the development of future clinical trials where ALT may be used as an adjunct to T cell-dependent therapies in primary CNS malignancy (e.g., BRiTE, NCT04903795). Ongoing process development work to identify the ideal combination, schedule, and doses of co-culture cytokines will be required to generate the optimal ALT product.

Materials and Methods

Sex as a biological variable

For pre-clinical evaluation in immunocompetent mice, our study exclusively used female animals as the CT-2A tumor line was established in female mice[51]. Superior engraftment of human hematopoietic stem cells has also been observed in female NOD-*scid* gamma (NSG) mice[52]. Evaluation of clinical samples from volunteer donors and patients with glioblastoma used hPBMCs from both male and female subjects (breakdown shown in **Table 1**).

Mice

All animal experiments were performed under an approved Duke University Institutional Animal Care and Use Committee (IACUC) experimental protocol (ID: A163-21-08). Six-to ten-week-old C57BL/6J, CD45.1 (B6.SJL-Ptprc^{a} Pepc^{b}/BoyJ) and NSG mice were purchased from Jackson laboratories. Animals were housed in a temperature and humidity-controlled pathogen-free environment and kept under a 12-hour lighting cycle at the Cancer Center Isolation Facility (CCIF) at Duke University, NC, USA. Regular checks for animal welfare were made by study investigators and CCIF staff as per IACUC protocols.

Cell lines

C57BL/6 syngeneic CT2A was originally provided by Robert L. Martuza (Massachusetts General Hospital). Generation of stably transfected sublines was performed in-house, and their use has been described in previous studies[9]. Similarly, U87-MG was obtained from the ATCC and transfected in-house to stably express EGFRvIII . Their generation and usage has also been described in prior studies by our group[26]. All cell lines have been authenticated and evaluated to be contaminant free via IDEXX Laboratories. Both CT2A and U87MG lines were maintained in culture using complete DMEM (Gibco, 11995-065, 10% FBS) and passaged using 0.05% Trypsin, EDTA (Gibco, 25300-054).

Murine lymphocyte culturing

Expansion of murine CD3^{+} cells was performed by first harvesting spleens from healthy 6–10-week-old genetically identical mice. Spleens were disrupted over a 70-µm strainer before re-suspension in ACK lysis buffer (Quality Biological, 118-156-101) for 2 minutes before neutralization. Cells were then re-suspended at a concentration of 2 x 10^{6} cells/mL in complete T cell medium supplemented with either 100 IU/mL IL-2 (ProLeukin), or 20 ng/mL IL-7 (PeproTech, 217-17). Complete T cell medium consists of RPMI 1640 (Sigma-Aldrich, R8758) with 10% FBS and supplemented with 1:100 Minimum Essential Medium Non-Essential Amino Acids (MEM NEAA, Gibco, 1114050), 1:100 Sodium Pyruvate (Gibco, 11360070), 1:100 L-Glutamine (Gibco, 25030081), 1:100 Pen-Strep (Gibco, 15140122), 1:1000 2-Mercaptoethanol (ThermoScientific, 21985023) and 1:1000 Gentamicin (Gibco, 1570060). After collection, cells were stimulated with 2 µg/mL Concanavalin A (Sigma-Aldrich, C5275). Cells were maintained in 24-well tissue culture plates (Corning Falcon) and split every 2-3 days to maintain concentration at 1-2 x 10^{6} cells/mL prior to usage for either ALT or flow cytometry.

Leukapheresis and human PBMC culturing

Human PBMCs were obtained by leukapheresis at the Duke Apheresis Unit (SOP-JHS-HDC-CL-023 “Leukapheresis Collection Procedure”) and transported to the Cell Processing facility (SOP-JHS-HDC-CL-011 “Leukapheresis Transport

and Receipt Procedure"). Samples used in this study were collected from patients or volunteers who provided written consent to undergo leukapheresis for the purposes of hPBMC expansion (**EXCEL:** Newly diagnosed GBM patients prior to RT and TMZ, EGFRvIII$^+$ Tumors, NCT02664363, Duke IRB #Pro00069444; **INTERCEPT:** Recurrent GBM patients, EGFRvIII$^+$ Tumors, NCT03283631, Duke IRB #Pro00083828; **ALPS:** Healthy volunteer donors, Duke IRB: #Pro00009403). Briefly, following leukapheresis, samples were diluted, underlayered with Ficoll (Histopaque-1077, Sigma-Aldrich, 10771), and spun to select for hPBMCs. Samples were then stored long term in liquid nitrogen storage and kept below -135°C. Cryopreserved PBMCs from healthy donors and from glioblastoma patients were then thawed into PrimeXV T-cell expansion media (FujiFilm) supplemented with 3% of human platelet lysate (hPL, Compass Biomedical) and pelleted at 300g for 10 min. The cell pellet was re-suspended in PrimeXV/3% hPL to a concentration of 1 x 10^6 cells/ml and 1 x 10^6 cells plated per well of a G-Rex 6M six well plate (Wilson-Wolf). Note: sample "Normal Donor #1" was plated at 3.6 x 10^5 cells/well and "Normal Donor #2" was plated at 9 x10^5 cells/well. For each sample, two wells were set up. One was supplemented with IL-2 at 300 IU/ml (BioTechne, BT-002-AFL) and the other was supplemented with IL-7 at 20ng/ml (PeproTech, 200-07). The cells were activated with 100µl a-CD3/a-CD8 nanoparticles (TransAct, Miltenyi, 130-111-160) according to the manufacturers protocol. The plates were incubated at 37ºC and 5% CO2. On culture day 3, TransAct was inactivated by adding 10x volume of complete media. On culture day 7, 90% of the media was removed, the cells counted, a small aliquot removed for flow cytometry analysis, the culture split to 1 x10^6 cells/cm^2 and fresh media added to a total of 100 ml. Cultures were monitored daily for lactate levels and media changed when lactate levels reached 15 mM. On culture day 14, 90% of media was removed, the cells re-suspended and counted and analyzed by flow cytometry.

Tumor inoculation

All tumor studies in this report placed tumors intracranially in mice and followed protocols described previously[53]. Briefly, we collected tumor cells in logarithmic growth by first detaching them from their culture flasks using 0.05% Trypsin, EDTA (Gibco, 25300-054). Cells were then suspended in sterile phosphate buffered saline (PBS, Gibco, 10010-023) before being mixed in a 1:1 ratio with 10% methylcellulose (Sigma, M-0512). The tumor-methylcellulose mixture was then loaded into a 250µL Hamilton syringe (Hamilton company, 81120) with a 25-gauge needle attached. Mice were anesthetized with isoflurane before being placed into a stereotactic frame. The scalp was sterilized, and a midline incision was made to visualize the bregma. The loaded syringe was then positioned 2mm lateral to the right of the bregma and lowered 5mm through the skull, before being retracted 1mm to form a pocket for tumor cell inoculation. This pocket was then infused with 5µL of tumor cells at 120µL per minute. For tumor studies using CT2AvIII, 3 x 10^4 cells were infused, while studies using U87vIII infused 2.5 x 10^4 cells per mouse. Tumor infusate was allowed to settle in the intracranial pocket for 45 seconds, before the needle was withdrawn. The injection site was then closed with bone wax and the wound was stapled closed. Mice were allowed to recover before cages were replaced.

In vivo adoptive lymphocyte transfer and antibody administration

For adoptive lymphocyte transfer in this study, cells that had been expanded as described in the murine lymphocyte culturing section were collected and suspended in PBS at a concentration of 1 x 10^8 cells/mL. 100 µL (equivalent to a dose of 1 x 10^7 cells per mouse) was administered via retro-orbital intravenous injection using an Ultra-Fine Lo-Dose insulin syringe (BD, 324703).

Antibody administration of anti-VLA-4 (clone PS/2, Bio X Cell #BE0071), anti-4-1BB (clone LOB12.3, Bio X Cell #BP0169), anti-PD-1 (clone 29F.1A12, Bio X Cell, #BE0273) and anti-CTLA-4 (clone 9D9, Bio X Cell, #BE0164) were performed as part of this study. Intraperitoneal doses consisted of 200 µg antibody made up to 200 µL with PBS and given as described in study descriptions. For intracranial administration (anti-VLA-4 only), 2 µg antibody was made up to 20 µL with PBS and given in a similar fashion to tumor inoculation above, using the same injection site through which tumors were implanted.

hEGFRvIII:CD3 BRiTE (lot #201905) was manufactured at CellDex therapeutics to cGMP standards for a planned clinical trial (NCT04903795) and has been described in detail previously[9]. Stock solution of 0.5 mg/mL was maintained at -80°C until use. For administration to animals, 100 µL (equivalent to 50 µg per mouse) was given via retro-orbital intravenous injection using the same insulin syringe as above.

Tissue processing and flow cytometry

Procedures for tissue processing and flow cytometry are based on our previously published protocols[54]. Briefly, mice were anesthetized with isoflurane before undergoing cardiac puncture and perfusion with PBS. Following perfusion, brain tissue, bone marrow, spleen and lungs were collected and prepared for staining (dependent on experimental design). To isolate tumors, brains were divided into tumor-bearing hemispheres (typically right hemisphere) and non-tumor-bearing hemispheres (left). At the point of collection, visual confirmation of tumor presence in hemisphere was performed. Collection of blood was performed either via retro-orbital eye bleeds or cardiac puncture prior to perfusion. After collection, tissue was homogenized in digestion medium consisting of 0.05mg/mL Liberase DL (Roche, 5401160001), 0.05mg/mL Liberase TL (Roche, 5401020001) and 0.2mg/mL DNAse I (Roche, 10104159001), in HBSS with calcium and magnesium (Gibco, 14175095). Tissue in digestion buffer placed in a dounce tissue homogenizer (Wheaton, 62400-620) and disaggregated into a cell suspension following 5-10 strokes with a loose-fitting (A-size pestle). This suspension was then incubated for 15 minutes at 37°C before filtering through a 70-µm strainer. Note: lung tissue was placed in a shaker for 45 minutes with digestion buffer to ensure cell suspension. Femurs were removed from mice and bone marrow removed by centrifugation at 10,000xg for 30 seconds. After centrifugation, cells were re-suspended in ACK lysis buffer (Quality Biological, 118-156-101) for 2 minutes before neutralization. Myelin was removed from brain tissue by 30 minutes of centrifugation with 30% Percoll (Sigma Aldrich, P1644) with no brake. After long centrifuge, the myelin layer was carefully aspirated, and the remaining cell pellet resuspended at a concentration of 1-2 x 10^7 cells/mL in PBS. Cells maintained in culture for removed from culture vessels and pelleted at 500g for 5 minutes and similarly resuspended in PBS for flow cytometry.

Before panel staining, Live/Dead Aqua (1:200, ThermoFisher, L34966) was added and co-incubated for 30 minutes at 4°C to assess for viability. Brilliant Stain buffer (BD, 563794) was added prior to addition of panels (antibodies listed in **Supplementary Table 1**). Staining was again performed by co-incubation for 30 minutes at 4°C before fixation in flow buffer (PBS, 1% BSA, 0.5 mM EDTA) with 1% formaldehyde. Prior to flow cytometry, counting beads (Invitrogen, C36950) were added to a fixed volume (i.e., 10 µL beads to 300 µL sample in fix buffer). Determination of counts per weight was performed by the following calculations:

$$Cell\ Concentration\ (per\ \mu L) = \frac{Number\ of\ acquired\ cells}{Number\ of\ acquired\ beads}\ x\ \frac{Number\ of\ beads\ added\ to\ sample}{Total\ volume\ of\ analyzed\ sample}$$

$$Normalized\ count\ (per\ gram) = \frac{Cell\ concentration\ x\ Total\ volume\ of\ analyzed\ sample}{Fraction\ of\ sample\ stained\ x\ Tissue\ weight}$$

Flow cytometry was performed on a LSR Fortessa (BD) using FACS Diva Software v.9, BD Biosciences and analyzed with FlowJo v.10 (Tree Star).

Cytotoxicity assays

Assessments of cytotoxicity *in vitro* were performed using a 24-hour co-culture with target tumor cells and T cells before staining for viability. Tumor cells were initially labelled with a viability dye (Cell Trace Violet, ThermoFisher, C34557) before being added to a 96-well plate (1 x 10^4 cells per well). T cells were then added to each well at a 10:1 ratio (1 x 10^5 cells per well). Antibody under evaluation was added at a starting concentration of 10 µg/mL in the first row, before 10-fold serial dilutions were added to subsequent rows. The final row did not have any antibody added and served as a control for any background cytotoxicity. After 24 hours of co-culture, cells were trypsinized, and re-suspended in 115 µL flow buffer with 10 µL of counting beads added per well (Invitrogen, C36950, 125 µL total per well). Plates were then analyzed using a high-throughput reader attached to a LSR Fortessa (BD) and data acquired as per usual flow cytometry procedures. Percentage viability was assessed based on control well bead-normalized counts representing 100% tumor viability/no antibody effect.

Statistics and reproducibility

Experimental results are presented as mean ± SEM unless otherwise stated. Statistical tests for all studies were completed using GraphPad v.8.4.3 (Prism). For comparisons in a single graph, unpaired two-tailed Mann-Whitney U test was used. Asterisks were appended to graphs to represent the significance level of any difference (*p<0.05, **p≤0.01, ***p<0.001, ****p<0.0001, p>0.05 not significant). Sample sizes were selected due to practical considerations, with no formal power calculations performed prior to experiments. Efficacy studies following animals for survival were assessed for significance using a log-rank (Mantel-Cox) test. Independent efficacy study results were pooled if the effect of replication did not cause significant variation as assessed by two-way ANOVA. All animals were randomized within genotype prior to treatment following tumor implantation. Survival was monitored with the assistance of technicians from the Duke Division of Laboratory Animal Resources (DLAR) who were blinded to study groups and followed animals to endpoint.

Graphical illustrations

Experimental outlines in Figs. 1, 2, 3, S1, S3 and S4 were created with BioRender.com and exported under a paid license.

Data Availability

Values for underlying data and reported means for all figures are available in the supporting data values file.

References

1 Belmontes, B. *et al.* Immunotherapy combinations overcome resistance to bispecific T cell engager treatment in T cell-cold solid tumors. *Science Translational Medicine* **13**, eabd1524 (2021). https://doi.org/doi:10.1126/scitranslmed.abd1524

2 Woroniecka, K. I. *et al.* 4-1BB Agonism Averts TIL Exhaustion and Licenses PD-1 Blockade in Glioblastoma and Other Intracranial Cancers. *Clinical cancer research : an official journal of the American Association for Cancer Research* **26**, 1349-1358 (2020). https://doi.org/10.1158/1078-0432.Ccr-19-1068

3 Baeuerle, P. A. & Wesche, H. T-cell-engaging antibodies for the treatment of solid tumors: challenges and opportunities. *Curr Opin Oncol* **34**, 552-558 (2022). https://doi.org/10.1097/cco.0000000000000869

4 Chongsathidkiet, P. *et al.* Sequestration of T cells in bone marrow in the setting of glioblastoma and other intracranial tumors. *Nat Med* **24**, 1459-1468 (2018). https://doi.org/10.1038/s41591-018-0135-2

5 Maddison, K. *et al.* Low tumour-infiltrating lymphocyte density in primary and recurrent glioblastoma. *Oncotarget* **12**, 2177-2187 (2021). https://doi.org/10.18632/oncotarget.28069

6 Reardon, D. A. *et al.* Effect of Nivolumab vs Bevacizumab in Patients With Recurrent Glioblastoma: The CheckMate 143 Phase 3 Randomized Clinical Trial. *JAMA Oncology* **6**, 1003-1010 (2020). https://doi.org/10.1001/jamaoncol.2020.1024

7 Omuro, A. *et al.* Radiotherapy combined with nivolumab or temozolomide for newly diagnosed glioblastoma with unmethylated MGMT promoter: An international randomized phase III trial. *Neuro-oncology* **25**, 123-134 (2023). https://doi.org/10.1093/neuonc/noac099

8 Lim, M. *et al.* Phase III trial of chemoradiotherapy with temozolomide plus nivolumab or placebo for newly diagnosed glioblastoma with methylated MGMT promoter. *Neuro-oncology* **24**, 1935-1949 (2022). https://doi.org/10.1093/neuonc/noac116

9 Gedeon, P. C. *et al.* A Rationally Designed Fully Human EGFRvIII:CD3-Targeted Bispecific Antibody Redirects Human T Cells to Treat Patient-derived Intracerebral Malignant Glioma. *Clinical cancer research : an official journal of the American Association for Cancer Research* **24**, 3611-3631 (2018). https://doi.org/10.1158/1078-0432.Ccr-17-0126

10 Woroniecka, K. *et al.* T-Cell Exhaustion Signatures Vary with Tumor Type and Are Severe in Glioblastoma. *Clinical cancer research : an official journal of the American Association for Cancer Research* **24**, 4175-4186 (2018). https://doi.org/10.1158/1078-0432.CCR-17-1846

11 Agliardi, G. *et al.* Intratumoral IL-12 delivery empowers CAR-T cell immunotherapy in a pre-clinical model of glioblastoma. *Nature Communications* **12**, 444 (2021). https://doi.org/10.1038/s41467-020-20599-x

12 Leonard, J. P. *et al.* Effects of single-dose interleukin-12 exposure on interleukin-12-associated toxicity and interferon-gamma production. *Blood* **90**, 2541-2548 (1997).

13 Zhang, L. *et al.* Tumor-infiltrating lymphocytes genetically engineered with an inducible gene encoding interleukin-12 for the immunotherapy of metastatic melanoma. *Clinical cancer research : an official journal of the American Association for Cancer Research* **21**, 2278-2288 (2015). https://doi.org/10.1158/1078-0432.Ccr-14-2085

14 Bagley, S. J. *et al.* Intrathecal bivalent CAR T cells targeting EGFR and IL13Rα2 in recurrent glioblastoma: phase 1 trial interim results. *Nature Medicine* (2024). https://doi.org/10.1038/s41591-024-02893-z

15 Choi, B. D. *et al.* Intraventricular CARv3-TEAM-E T Cells in Recurrent Glioblastoma. *New England Journal of Medicine* (2024). https://doi.org/10.1056/NEJMoa2314390

16 Bagley, S. J. *et al.* Repeated peripheral infusions of anti-EGFRvIII CAR T cells in combination with pembrolizumab show no efficacy in glioblastoma: a phase 1 trial. *Nature Cancer* (2024). https://doi.org/10.1038/s43018-023-00709-6

17 Ross, S. H. & Cantrell, D. A. Signaling and Function of Interleukin-2 in T Lymphocytes. *Annu Rev Immunol* **36**, 411-433 (2018). https://doi.org/10.1146/annurev-immunol-042617-053352

18 Yang, S., Archer, G. E., Flores, C. E., Mitchell, D. A. & Sampson, J. H. A cytokine cocktail directly modulates the phenotype of DC-enriched anti-tumor T cells to convey potent anti-tumor activities in a murine model. *Cancer immunology, immunotherapy : CII* **62**, 1649-1662 (2013). https://doi.org/10.1007/s00262-013-1464-0

19 Chen, D., Tang, T. X., Deng, H., Yang, X. P. & Tang, Z. H. Interleukin-7 Biology and Its Effects on Immune Cells: Mediator of Generation, Differentiation, Survival, and Homeostasis. *Front Immunol* **12**, 747324 (2021). https://doi.org/10.3389/fimmu.2021.747324

20 ElKassar, N. & Gress, R. E. An overview of IL-7 biology and its use in immunotherapy. *J Immunotoxicol* **7**, 1-7 (2010). https://doi.org/10.3109/15476910903453296

21 Pang, N. *et al.* IL-7 and CCL19-secreting CAR-T cell therapy for tumors with positive glypican-3 or mesothelin. *J Hematol Oncol* **14**, 118 (2021). https://doi.org/10.1186/s13045-021-01128-9

22 Campian, J. L. *et al.* Long-Acting Recombinant Human Interleukin-7, NT-I7, Increases Cytotoxic CD8 T Cells and Enhances Survival in Mouse Glioma Models. *Clinical Cancer Research* **28**, 1229-1239 (2022). https://doi.org/10.1158/1078-0432.Ccr-21-0947

23 Hickey, W. F., Hsu, B. L. & Kimura, H. T-lymphocyte entry into the central nervous system. *Journal of Neuroscience Research* **28**, 254-260 (1991). https://doi.org/https://doi.org/10.1002/jnr.490280213

24 Hinrichs, C. S. *et al.* IL-2 and IL-21 confer opposing differentiation programs to CD8+ T cells for adoptive immunotherapy. *Blood* **111**, 5326-5333 (2008). https://doi.org/10.1182/blood-2007-09-113050

25 Markley, J. C. & Sadelain, M. IL-7 and IL-21 are superior to IL-2 and IL-15 in promoting human T cell–mediated rejection of systemic lymphoma in immunodeficient mice. *Blood* **115**, 3508-3519 (2010). https://doi.org/10.1182/blood-2009-09-241398

26 Choi, B. D. *et al.* Systemic administration of a bispecific antibody targeting EGFRvIII successfully treats intracerebral glioma. *Proceedings of the National Academy of Sciences* **110**, 270-275 (2013). https://doi.org/10.1073/pnas.1219817110

27 Kohlmeier, J. E. *et al.* The chemokine receptor CCR5 plays a key role in the early memory CD8+ T cell response to respiratory virus infections. *Immunity* **29**, 101-113 (2008). https://doi.org/10.1016/j.immuni.2008.05.011

28 Ray, S. J. *et al.* The collagen binding alpha1beta1 integrin VLA-1 regulates CD8 T cell-mediated immune protection against heterologous influenza infection. *Immunity* **20**, 167-179 (2004). https://doi.org/10.1016/s1074-7613(04)00021-4

29 Ley, K. & Kansas, G. S. Selectins in T-cell recruitment to non-lymphoid tissues and sites of inflammation. *Nature reviews. Immunology* **4**, 325-335 (2004). https://doi.org/10.1038/nri1351

30 Nolz, J. C., Starbeck-Miller, G. R. & Harty, J. T. Naive, effector and memory CD8 T-cell trafficking: parallels and distinctions. *Immunotherapy* **3**, 1223-1233 (2011). https://doi.org/10.2217/imt.11.100

31 Rice, G. P. A., Hartung, H.-P. & Calabresi, P. A. Anti-α4 integrin therapy for multiple sclerosis. *Mechanisms and rationale* **64**, 1336-1342 (2005). https://doi.org/10.1212/01.Wnl.0000158329.30470.D0

32 Sehr, T. *et al.* New insights into the pharmacokinetics and pharmacodynamics of natalizumab treatment for patients with multiple sclerosis, obtained from clinical and in vitro studies. *Journal of Neuroinflammation* **13**, 164 (2016). https://doi.org/10.1186/s12974-016-0635-2

33 Mittelbrunn, M. *et al.* VLA-4 integrin concentrates at the peripheral supramolecular activation complex of the immune synapse and drives T helper 1 responses. *Proceedings of the National Academy of Sciences* **101**, 11058-11063 (2004). https://doi.org/doi:10.1073/pnas.0307927101

34 Miao, H. *et al.* EGFRvIII-specific chimeric antigen receptor T cells migrate to and kill tumor deposits infiltrating the brain parenchyma in an invasive xenograft model of glioblastoma. *PLoS One* **9**, e94281 (2014). https://doi.org/10.1371/journal.pone.0094281

35 Cieri, N. *et al.* IL-7 and IL-15 instruct the generation of human memory stem T cells from naive precursors. *Blood* **121**, 573-584 (2013). https://doi.org/10.1182/blood-2012-05-431718

36 Kondo, T. *et al.* Generation and application of human induced-stem cell memory T cells for adoptive immunotherapy. *Cancer science* **109**, 2130-2140 (2018). https://doi.org/10.1111/cas.13648

37 Singh, K. *et al.* For whom the T cells troll? Bispecific T-cell engagers in glioblastoma. *J Immunother Cancer* **9** (2021). https://doi.org/10.1136/jitc-2021-003679

38 Tomaszewski, W., Sanchez-Perez, L., Gajewski, T. F. & Sampson, J. H. Brain Tumor Microenvironment and Host State: Implications for Immunotherapy. (2019). https://doi.org/10.1158/1078-0432.CCR-18-1627

39 Mrdjen, D. *et al.* High-Dimensional Single-Cell Mapping of Central Nervous System Immune Cells Reveals Distinct Myeloid Subsets in Health, Aging, and Disease. *Immunity* **48**, 380-395.e386 (2018). https://doi.org/10.1016/j.immuni.2018.01.011

40 Kitazawa, H. *et al.* IL-7 activates alpha4beta1 integrin in murine thymocytes. *The Journal of Immunology* **159**, 2259-2264 (1997). https://doi.org/10.4049/jimmunol.159.5.2259

41 Unsinger, J. *et al.* IL-7 Promotes T Cell Viability, Trafficking, and Functionality and Improves Survival in Sepsis. *The Journal of Immunology* **184**, 3768-3779 (2010). https://doi.org/10.4049/jimmunol.0903151

42 Sasaki, K., Pardee, A. D., Okada, H. & Storkus, W. J. IL-4 inhibits VLA-4 expression on Tc1 cells resulting in poor tumor infiltration and reduced therapy benefit. *European Journal of Immunology* **38**, 2865-2873 (2008). https://doi.org/https://doi.org/10.1002/eji.200838334

43 Sevenich, L. Turning "Cold" Into "Hot" Tumors-Opportunities and Challenges for Radio-Immunotherapy Against Primary and Metastatic Brain Cancers. *Front Oncol* **9**, 163 (2019). https://doi.org/10.3389/fonc.2019.00163

44 Wang, S.-Y. *et al.* Nonactivated and IL-7 cultured CD19-specific CAR T cells are enriched in stem cell phenotypes and functionally superior. *Blood Advances* **8**, 324-335 (2024). https://doi.org/10.1182/bloodadvances.2023010607

45 Zhou, J. *et al.* Chimeric antigen receptor T (CAR-T) cells expanded with IL-7/IL-15 mediate superior antitumor effects. *Protein Cell* **10**, 764-769 (2019). https://doi.org/10.1007/s13238-019-0643-y

46 Woroniecka, K. I., Rhodin, K. E., Chongsathidkiet, P., Keith, K. A. & Fecci, P. E. T-cell Dysfunction in Glioblastoma: Applying a New Framework. *Clin Cancer Res* **24**, 3792-3802 (2018). https://doi.org/10.1158/1078-0432.Ccr-18-0047

47 Elliott, L. H., Brooks, W. H. & Roszman, T. L. Cytokinetic basis for the impaired activation of lymphocytes from patients with primary intracranial tumors. *J Immunol* **132**, 1208-1215 (1984).

48 Löhr, M. *et al.* High-grade glioma associated immunosuppression does not prevent immune responses induced by therapeutic vaccines in combination with Treg depletion. *Cancer Immunology, Immunotherapy* **67**, 1545-1558 (2018). https://doi.org/10.1007/s00262-018-2214-0

49 Xu, X. J. *et al.* Multiparameter comparative analysis reveals differential impacts of various cytokines on CART cell phenotype and function ex vivo and in vivo. *Oncotarget* **7**, 82354-82368 (2016). https://doi.org/10.18632/oncotarget.10510

50 Vranjkovic, A., Crawley, A. M., Gee, K., Kumar, A. & Angel, J. B. IL-7 decreases IL-7 receptor alpha (CD127) expression and induces the shedding of CD127 by human CD8+ T cells. *Int Immunol* **19**, 1329-1339 (2007). https://doi.org/10.1093/intimm/dxm102

51 Martínez-Murillo, R. & Martínez, A. Standardization of an orthotopic mouse brain tumor model following transplantation of CT-2A astrocytoma cells. *Histol Histopathol* **22**, 1309-1326 (2007). https://doi.org/10.14670/hh-22.1309

52 Notta, F., Doulatov, S. & Dick, J. E. Engraftment of human hematopoietic stem cells is more efficient in female NOD/SCID/IL-2Rgc-null recipients. *Blood* **115**, 3704-3707 (2010). https://doi.org/10.1182/blood-2009-10-249326

53 Schaller, T. H. *et al.* First in human dose calculation of a single-chain bispecific antibody targeting glioma using the MABEL approach. *J Immunother Cancer* **8** (2020). https://doi.org/10.1136/jitc-2019-000213

54 Tomaszewski, W. H. *et al.* Broad immunophenotyping of the murine brain tumor microenvironment. *Journal of Immunological Methods* **499**, 113158 (2021). https://doi.org/https://doi.org/10.1016/j.jim.2021.113158

Tables

Table 1. Demographics of hPBMC samples taken from healthy volunteers and glioblastoma patients.

Characteristics	No. of control samples N = 5	No. of patient samples N = 6
Age		
Median	54.3	58.7
Range	43-55	37-63
Sex		
Male	2	4
Female	1	2
Unknown	2	0
Diagnosis		
IDHwt* Glioblastoma	NA	6
Newly Diagnosed	NA	4
Recurrent	NA	2
Steroid Status		
Naïve	NA	1
Experienced	NA	5

*IDHwt: Isocitrate Dehydrogenase wild-type

Figures

Figure 1. IL-7-expanded autologous T cells demonstrate enhanced accumulation within orthotopic glioblastoma models despite endogenous T cell sequestration in bone marrow.

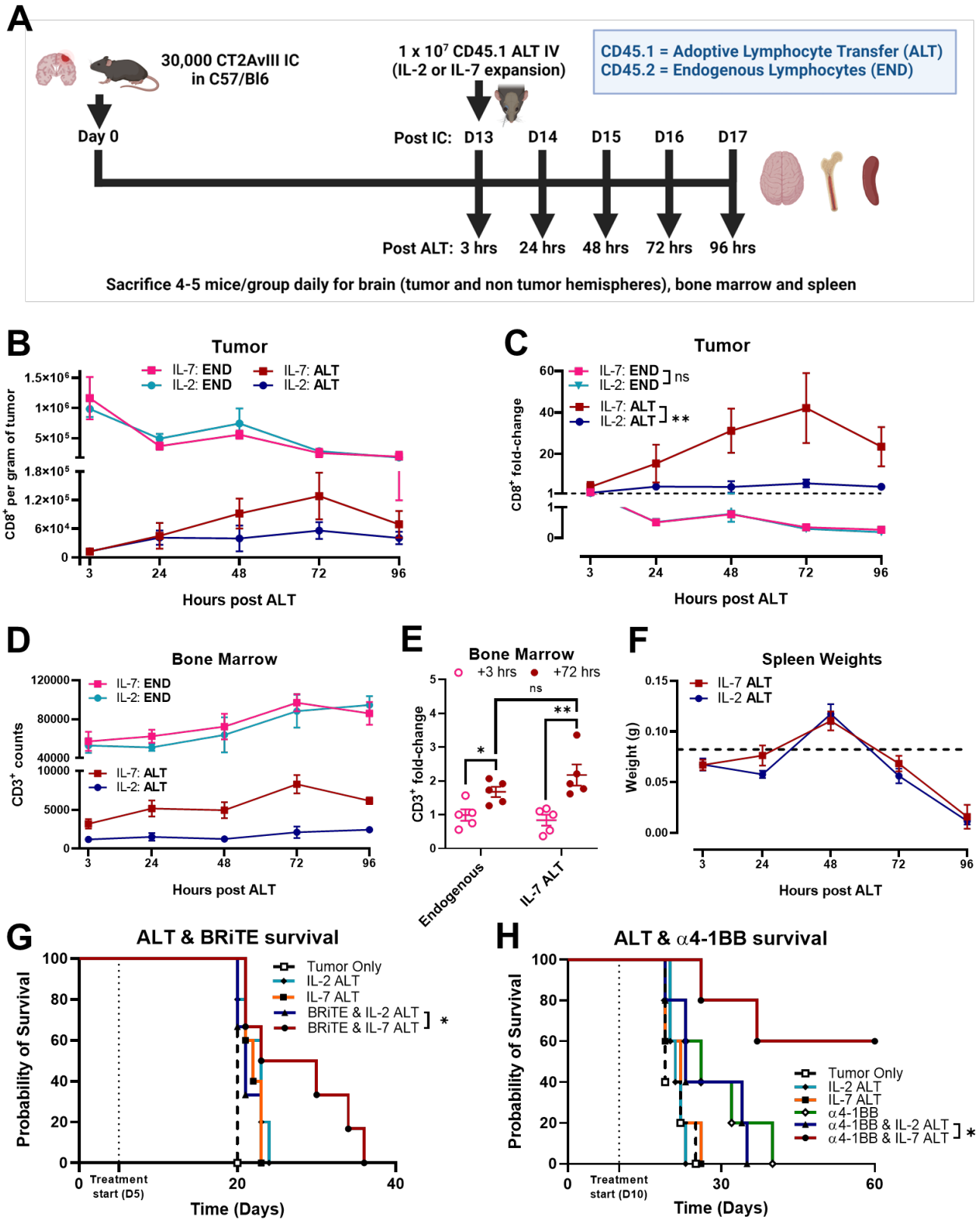

Figure 1. IL-7-expanded autologous T cells demonstrate enhanced accumulation within orthotopic glioblastoma models despite endogenous T cell sequestration in bone marrow.

(A) Study overview: C57BL/6 mice (n=4-5 mice per group per time point) were implanted with 3 x 10^4 cells of syngeneic glioma (CT-2AvIII) and treated with 1 x 10 IV^7 $CD45.1^+$ ALT on Day 13. Brain (sub-divided into tumor and non-tumor bearing hemispheres), bone marrow and spleen tissue were taken and analyzed each day for exogenous ($CD45.1^+$, ALT) and endogenous ($CD45.2^+$, END) CD3/4/8 counts. Spleen weights were also recorded to assess for involution.

(B & C) Weight-normalized counts and fold-change relative to Day 0 of exogenous $CD45.1^+CD8^+$ entry into the CNS over time. Sustained accumulation over time is observed specifically for tumor-bearing hemispheres across both co-culture conditions, with peak counts and fold-changes observed at 72 hours following administration. At 48- and 72-hours, fold-increase in IL-7 co-cultured exogenous $CD8^+$ entry was significantly greater than the IL-2 co-cultured exogenous $CD8^+$ lymphocytes. (48-hours hours IL-7 median 20.74x increase vs IL-2 median 1.423x, p=0.0317*, 72-hours IL-7 median 26.66 increase vs IL-2 median 4.291x, p=0.0159*, Mann-Whitney U. One way ANOVA between IL-7 ALT in tumor and all other conditions, p=0.0018**). Dashed line represents baseline (i.e., 1x). Endogenous T cell counts reduced over time in both tumor and non-tumor bearing CNS. IL-7 ALT; native population decreases to 0.23x of day 0 in IL-7 ALT tumor group (p=0.0159***)** and IL-2 ALT; native population falling to 0.32x of day 0 in IL-2 ALT group (p=0.0159*).

(D) Tracking of endogenous and exogenous lymphocyte counts in bone marrow showed that $CD3^+$ counts increased across all groups as animals approached endpoint. Rates were similar across treatment conditions.

(E) Fold-change in endogenous $CD45.2^+CD3^+$ cells (median fold-increase vs day 0: 1.73x, p=0.0317*) and $CD45.1^+CD3^+$ cells **(**average fold-increase vs day 0: 1.92x, p=0.0079****)** were similar at 72-hours following administration (p=0.2381).

(F) Evaluation of spleen sizes following ALT demonstrated similar dynamics in both treatment groups, with a transient increase in spleen sizes following ALT, over and above normal control weights (dashed line, 0.0823g, n=5), before resumption of involution.

(G) Evaluation of IL-7 and IL-2 ALT combined with hCD3:EGFRvIII BRiTE in NSG mice. Mice (n=5-6 per group) were implanted with 2.5 x 10^4 cells of U87vIII and treated with 5 x 10 IV^6 hPBMCs on day 5, with sequential BRiTE treatment (50µg IV) on days 5-9 (n=6 per group). BRiTE and IL-7 hPBMCs yielded a significantly increased survival benefit compared to combination therapy with IL-2 hPBMCs (p=0.0496*, chi-square test).

(H) Combination IL-7 ALT and anti-4-1BB therapy produced increased anti-tumor efficacy compared to IL-2 ALT and anti-4-1BB. C57BL/6 mice were implanted with 3 x 10^4 cells CT2AvIII (n=5/group) and treated with IV ALT & IP mAb on Day 10, (treatment start shown as dashed vertical line). IP mAb Injections were given every 3 days for 4 total cycles, IL-7 ALT & α4-1BB therapy demonstrated enhanced survival vs IL-2 ALT & α4-1BB (p=0.0132*).

Statistical analyses performed using two-tailed Mann-Whitney U and data presented as mean ± SEM unless otherwise specified. Experimental outlines generated using BioRender.com.

Figure 2. Increased accumulation of IL-7 expanded CD8⁺ lymphocytes in tumor consists of both central and effector memory phenotypes.

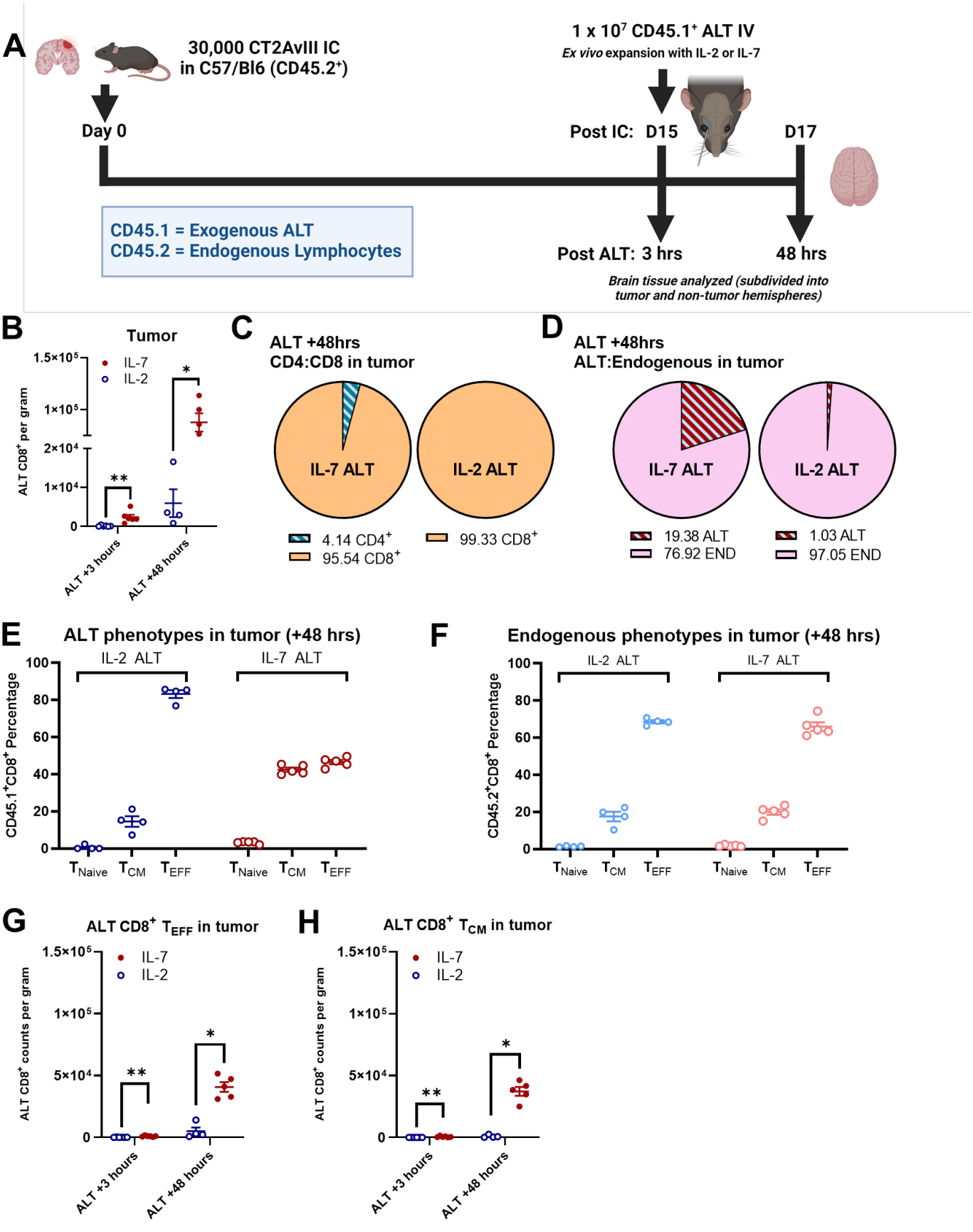

Figure 2. Increased accumulation of IL-7 expanded CD8+ lymphocytes in tumor consists of both central and effector memory phenotypes.

(A) Study overview: C57BL/6 mice (n=4-5/group) were implanted with 3 x 10^4 cells of syngeneic glioma (CT-2AvIII) and treated with 1 x 10 IV^7 $CD45.1^+$ ALT on Day 15. 3- and 48-hours following administration, brain tissue (sub-divided into tumor and non-tumor bearing hemispheres) was collected and exogenous ($CD45.1^+$) T cells were analyzed.

(B) Preferential entry of IL-7 expanded $CD45.1^+CD8^+$ lymphocytes were observed 3- and 48-hours following ALT in tumor hemispheres (IL-7 vs IL-2 3-hrs p=0.0022**, & 48-hrs p=0.0159*).

(C) Pie charts showing CD4:CD8 ratios in tumor tissue at ALT +48 hours for both expansion conditions. For both, >95% of exogenous T cells in the CNS at this time point were $CD8^+$.

(D) Proportions of exogenous ALT to endogenous T cells in tumor bearing hemispheres 48-hours following administration. IL-7 $CD45.1^+$ (ALT) cells made up approximately 20% of the T cell population (mean 19.4%, SD ±4.53%) whereas IL-2 ALT presence was near-negligible (mean 1.03%, SD ±0.35%).

(E) Phenotypic make up of exogenous ALT in tumor at 48-hours post administration found that IL-7 ALT resulted in a mixed phenotype of T_{CM} and T_{EFF} (IL-7 ALT T_{EFF} average 46.5%, SD ±2.32%. T_{CM} **a**verage 42.5%, SD ±2.20%), although T_{EFF} still was predominant. IL-2 ALT in tumor skewed towards T_{EFF}, akin to endogenous T cells.

(F) Endogenous lymphocyte phenotypic make up in tumor at 48-hours post administration of ALT. For both treatment groups, native phenotype ratios were similar, skewing primarily towards T_{EFF} subsets.

(G & H) Subset analysis of IL-7 expanded ALT cells which were found in tumor 48-hours post administration. Both IL-7 T_{CM} and IL-7 T_{EFF} entered the CNS in significantly greater numbers than IL-2 subsets (G, p=0.0159*; H**,** p=0.0159*).

Statistical analyses performed using two-tailed Mann-Whitney U and data presented as mean ± SEM unless otherwise specified. Experimental outlines generated using BioRender.com.

Figure 3. Expansion with IL-7 upregulates expression of the pro-migratory integrin VLA-4 on murine CD8⁺ cells, which is necessary for enhanced intra-tumoral accumulation.

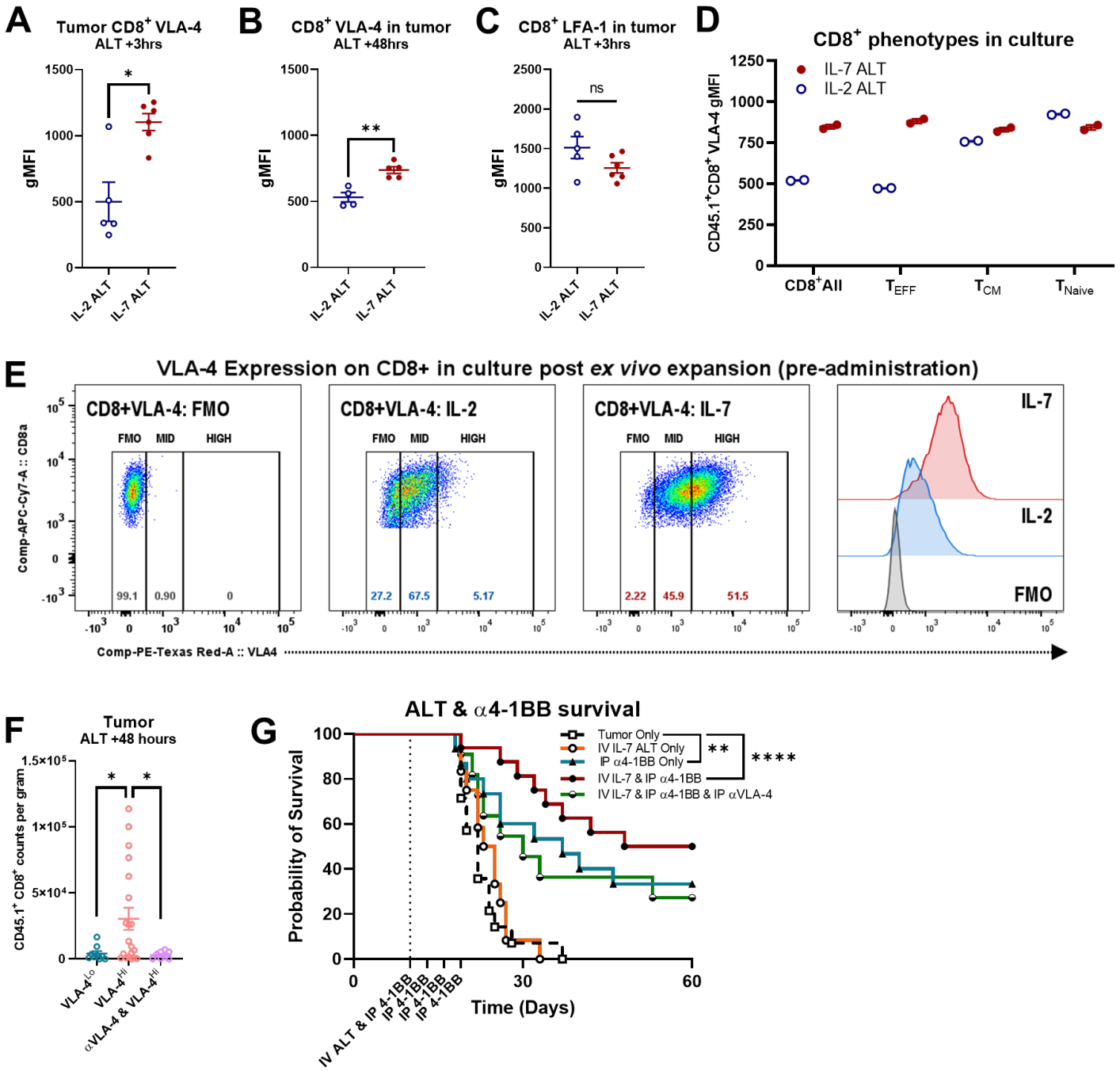

Figure 3. Expansion with IL-7 upregulates expression of the pro-migratory integrin VLA-4 on murine CD8+ cells, which is necessary for enhanced intra-tumoral accumulation.

(A & B) Analysis of VLA-4 expression on $CD8^+$ lymphocytes in tumor 3-hours and 48-hours post administration shows that IL-7 ALT cells had significantly increased geometric mean fluorescence intensity (gMFI) of VLA-4 (3-hours p=0.0173*, 48-hours p=0.0079**, experiment outline in figure 2, n=4-5/group)

(C) 3-hour comparison for LFA-1 shown, no significant difference clear in gMFI was observed between IL-2 ALT or IL-7 ALT (p=0.1775).

(D) Analysis of our ALT cellular product at the end of expansion found that IL-7 increased the proportion of T cells highly expressing VLA-4 compared to IL-2 (2 technical replicates per expansion condition).

(E) Representative gating strategy shown for VLA-4 expression

(F) Increased entry of $CD45.1^+CD8^+$ in tumor-bearing brain tissue following VLA-4^{Hi} ALT (VLA-4^{Hi} vs VLA-4^{Lo}, p=0.0491*) were abrogated by single-dose 200μg intraperitoneal Natalizumab (αVLA-4) blockade prior to ALT (VLA-4^{Hi} vs αVLA-4 & VLA-4^{Hi}, p=0.0428*, representation of 3 experiments shown, n=8-20/group). Counts were similar for VLA-4^{Lo} and αVLA-4 & VLA-4^{Hi} (p=0.9626).

(G) C57BL/6 mice were implanted IC with 3 x 10^4 CT2AvIII (representation of 3 experiments shown, n=10-15/group) and treated with IV ALT & IP mAb early on Day 10, along with 200μg of IP anti-4-1BB (treatment start shown as dashed vertical line, pooled experiments shown, n=11-15/group). One sub-group received 200μg Natalizumab IP 1 hour prior to IV ALT. IP mAb Injections were given every 3 days for 4 total cycles, IL-7 ALT & α4-1BB therapy demonstrated greatest survival benefit (median survival 54 days), p<0.0001**** vs tumor only, compared to monotherapy with α4-1BB only (median survival 37 days), p=0.0068* vs tumor only, or IL-7 ALT alone (median survival 24 days), p=0.5655 vs tumor only. Administration of intraperitoneal Natalizumab (αVLA-4, 200μg) 1 hour prior to ALT abrogated the enhanced survival benefit, and median survival (30 days) fell to below α4-1BB monotherapy.

Survival comparisons performed via Chi-Squared test. Other statistical analyses performed using two-tailed Mann-Whitney U and data presented as mean ± SEM unless otherwise specified. Experimental outlines generated using BioRender.com.

Figure 4. VLA-4 expression is increased on endogenous T cells in tumor.

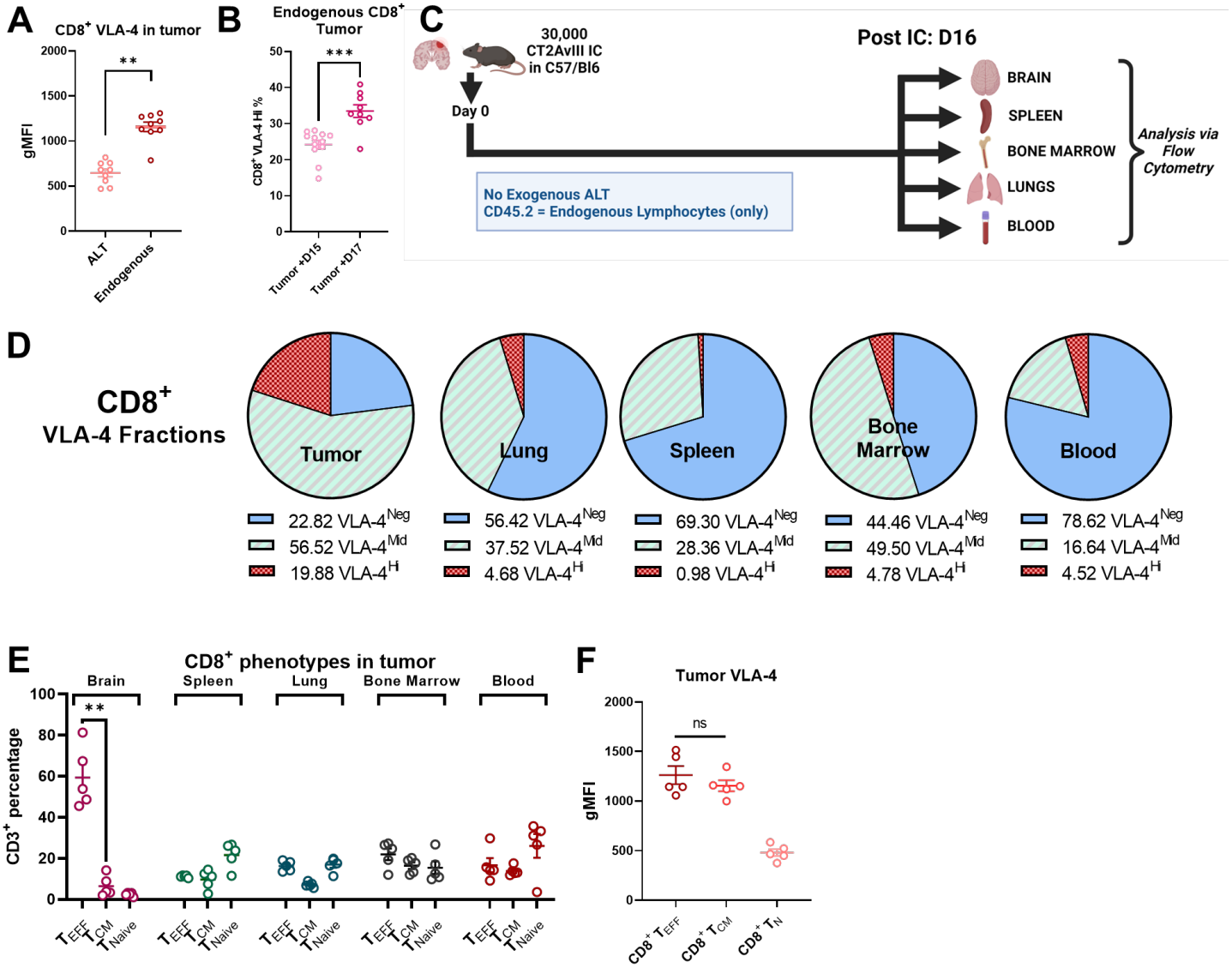

Figure 4. VLA-4 expression is increased on endogenous T cells in tumor.

(A) VLA-4 expression on endogenous IC $CD8^+$ T cells was significantly increased compared to ALT $CD8^+$ T cells in tumor (p=0.0039*, n=9/group, Wilcoxon matched-pairs, experiment outline in figure 2 for **A & B**).

(B) VLA-4 expression on endogenous $CD8^+$ cells specifically and significantly increased in the tumor bearing hemisphere between 15- and 17-days post implantation (implant +D15 vs implant +D17, tumor hemisphere, p=0.0007***, non-tumor hemisphere, p=0.3824).

(C) Study overview: C57BL/6 mice were implanted with 3 x 10^4 cells of syngeneic glioma (CT-2AvIII) which were allowed to establish for 16-days. No ALT was used for this analysis. At the 16-day timepoint, brain tissue, spleen, bone marrow, lungs and blood were collected and endogenous ($CD45.2^+$) T cells were analyzed (n=5/group).

(D) Evaluation of VLA-4^{Neg}, VLA-4^{Mid} and VLA-4^{Hi} fractions in different compartments found a found a larger VLA-4^{Hi} population in the brain compared to all other tested compartments (VLA-4^{Hi} mean fraction in brain 19.88%, SD ±6.27%, n=5).

(E) Phenotypic analysis of $CD8^+$ lymphocytes in compartments throughout the body found similar fractions aside from brain in which significantly more numbers of $CD8^+$ T_{EFF} cells compared to T_{CM} (p=0.0079**) were detected.

(F) VLA-4 gMFI on CD8+ T_{EFF}, T_{CM} and T_N subsets at the same timepoints in brain tumor hemispheres. No significant difference between $CD8^+$ T_{EFF} and T_{CM} subsets were observed (p=0.6905)

Statistical analyses performed using two-tailed Mann-Whitney U and data presented as mean ± SEM unless otherwise specified. Experimental outlines generated using BioRender.com.

Figure 5. Intracranial VLA-4 blockade enhances intratumoral T cell accumulation but does not enhance survival and reduces the cytotoxicity of T cell dependent immunotherapies.

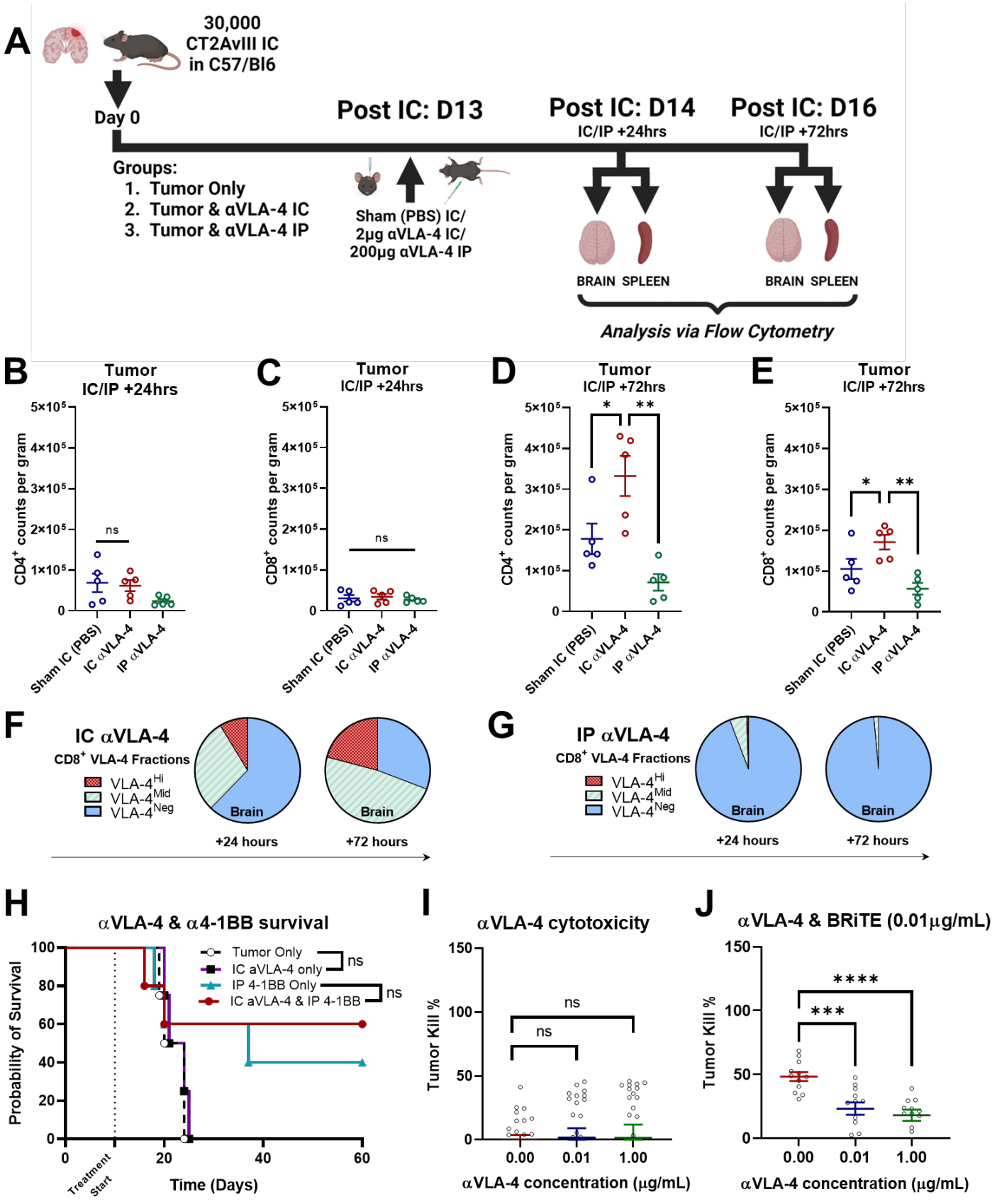

Figure 5. Intracranial VLA-4 blockade enhances intratumoral T cell accumulation but does not enhance survival and reduces the cytotoxicity of T cell dependent immunotherapies.

(A) Study overview to evaluate IC VLA-4 blockade. C57BL/6 mice (n=5/group) were implanted IC with 3 x 10^4 cells of syngeneic glioma (CT-2AvIII) which were allowed to establish for 13-days. On day 13, mice received either sham IC injection with PBS, 2μg of Natalizumab (αVLA-4) IC, or 200μg Natalizumab (αVLA-4) IP. Brain tissue and spleens were then analyzed 24- and 72-hours following administration.

(B) IC $CD4^+$ counts 24-hours following administration of IC (2μg) or IP (200μg) αVLA-4 or sham IC PBC controls and **(C)** IC $CD8^+$ counts 72-hours post-treatment. At this earlier timepoints, no significant changes in populations were observed between sham IC and IP αVLA-4 ($CD4^+$ sham IC vs IC αVLA-4, p=0.222; $CD8^+$ sham IC vs IC αVLA-4, p=0.8413.)

(D) IC $CD4^+$ counts 72-hours following administration of IC (2μg) or IP (200μg) αVLA-4 or sham IC PBC controls and **(E)** IC $CD8^+$ counts 72-hours post-treatment. Significant increases in both compared to sham IC and IP αVLA-4 ($CD4^+$ sham IC vs IC αVLA-4, p=0.0317*; $CD8^+$ sham IC vs IC αVLA-4, p=0.0317*.)

(F) VLA-4 gMFI fractions at 24-hrs and **(G)** 72-hrs shown following IC or IP αVLA-4 administration. IC αVLA-4 transiently decreased the IC VLA-4^{Hi} fraction, while IP maintained low levels of VLA-4 expression throughout.

(H) C57BL/6 mice (n=4-5/group) were implanted with 3 x 10^4 cells of syngeneic glioma (CT-2AvIII) and treated with 2μg Natalizumab (αVLA-4 mAb) IC on Day 10 (treatment start shown as dashed vertical line) or 200μg IP α4-1BB as a monotherapy or in combination (treatment on D10, D13, D16 & D19). No significant difference in survival was seen compared to tumor only controls if treating with IC αVLA-4 monotherapy, or when adding IC αVLA-4 to IP α4-1BB vs IP α4-1BB monotherapy.

(I) *In Vitro* cytotoxicity assay with progressively increasing αVLA-4 concentrations and co-cultured with tumor cells (U87vIII) and hPBMCs. Tumor cells were labelled with cell-trace violet after 24 hours of co-culture and analyzed via flow to assess viability. Increasing concentrations of αVLA-4 did not demonstrate any increased anti-tumor cytotoxicity (pooled experiments, n=24/dose).

(J) *In Vitro* cytotoxicity assay with progressively increasing αVLA-4 concentrations and hCD3:EGFRvIII BRiTE EC_{50} (BRiTE concentration 0.01μg/mL). BRiTE was co-cultured with tumor cells (U87vIII) and hPBMCs. Tumor cells were labelled with cell-trace violet after 24 hours of co-culture and analyzed via flow to assess viability. These doses were used for assessment of αVLA-4 impact on BRiTEs ability to form a cytotoxic immune synapse between tumor cell and lymphocyte. Addition of αVLA-4 to co-culture with BRiTE at previously established EC_{50} concentrations reduced tumor cytotoxicity (0μg/mL αVLA-4 vs 1μg/mL αVLA-4, tumor kill 48.45% vs 20.37% respectively, p<0.0001****, n=12/dose).

Survival comparisons performed via Chi-Squared test. Statistical analyses performed using two-tailed Mann-Whitney U and data presented as mean ± SEM unless otherwise specified. Experimental outlines generated using BioRender.com.

Figure 6. IL-7 expansion of hPBMCs from healthy volunteers and patients with glioblastoma enhances lymphocytic VLA-4 expansion compared to IL-2.

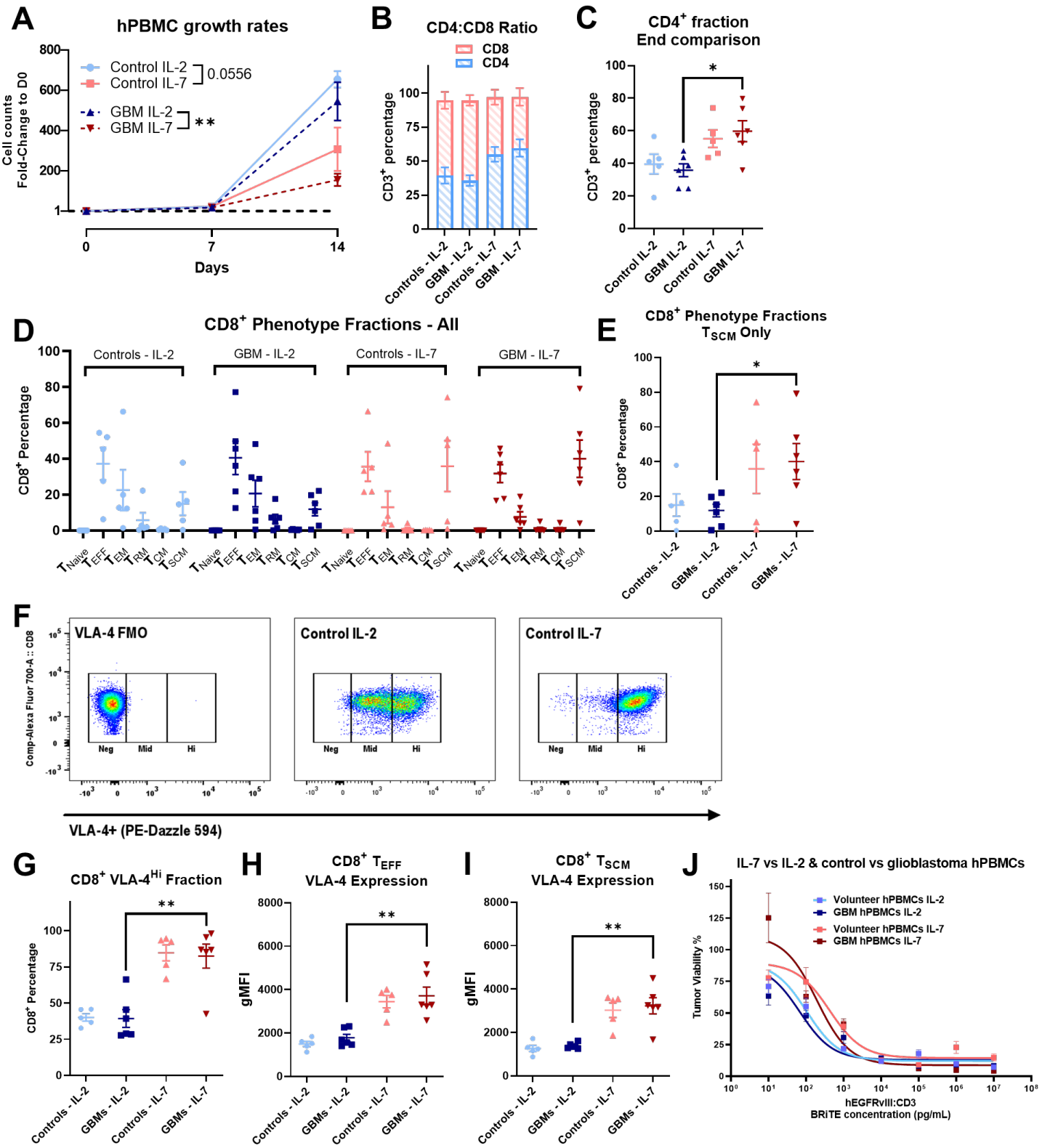

Figure 6. IL-7 expansion of hPBMCs from healthy volunteers and patients with glioblastoma enhances lymphocytic VLA-4 expansion compared to IL-2.

(A) hPBMC growth rates for IL-2 vs IL-7 co-culture from both GBM leukapheresis and healthy volunteer leukapheresis samples. hPBMCs from leukapheresis were thawed, stimulated with αCD3/αCD8 nanoparticles and expanded with 300IU/mL IL-2 or 20ng/mL IL-7 for 14 days. Counts and cell splits were performed on day 7 and day 14 post initiation of culture. n=5-6 samples per group. At expansion end, median fold-increase for donor controls was 225.2x vs 608.7x for IL-7 vs IL-2 respectively, p=0.0556 while median fold-increase for glioblastoma patient samples was 190.3x vs 558.1x for IL-7 vs IL-2 respectively, p=0.0043** (n=5-6/group).

(B) $CD4^+$:$CD8^+$ ratios for IL-2 vs IL-7 for donor controls and glioblastoma samples at end of expansion. IL-7 expansion skewed significantly more towards $CD4^+$ (~60:40 ratio of $CD4^+$:$CD8^+$) whereas IL-2 skewed towards $CD8^+$ ($CD4^+$:$CD8^+$ ~ 33:66).

(C) Comparison of $CD4^+$ fractions at end of expansion between groups. Both donor controls and glioblastoma patients cultured with IL-7 skewed more heavily towards $CD4^+$ (control IL-2 $CD4^+$ vs control IL-7 $CD4^+$: 42% vs 56.05%, p=0.026*, GBM IL-2 $CD4^+$ vs GBM IL-7 $CD4^+$: 37.2% vs 58.55%, p=0.0152*).

(D Overview of $CD8^+$ phenotype fractions at end of expansion process (Naïve (T_N), Effector (T_{EFF}), Effector Memory (T_{EM}), Resident Memory (T_{RM}), Central Memory (T_{CM}), Stem Cell Memory (T_{SCM}).

(E) Expansion with IL-7 significantly increased the fraction of $CD8^+$ T_{SCM} in the glioblastoma patient samples (GBM IL-2 $CD8^+$ T_{SCM} vs GBM IL-7 $CD8^+$ T_{SCM}: 13.05% vs 38.55%, p=0.026*).

(F & G) Gating strategy and VLA-4^{Hi} fraction shown for $CD8^+$ cells at the end of the expansion process. IL-7 approximately doubled the proportion of $CD8^+$ VLA-4^{Hi} compared to IL-2 expansion (control IL-2 $CD8^+$VLA-4^{Hi} vs control IL-7 $CD8^+$VLA-4^{Hi}: 39.1% vs 84.55%, p=0.0022**, GBM IL-2 $CD8^+$VLA-4^{Hi} vs GBM IL-7 $CD8^+$VLA-4^{Hi}: 34.1% vs 86.9%, p=0.0087**).

(H & I) Significant increases in VLA-4 gMFI on $CD8^+$ lymphocytes were restricted to $CD8^+$ T_{EFF} (control IL-2 $CD8^+$ T_{EFF} VLA-4 gMFI vs control IL-7 $CD8^+$ T_{EFF} VLA-4 gMFI: 1768 vs 3693, p=0.0022**, GBM IL-2 $CD8^+$ T_{EFF} VLA-4 gMFI vs GBM IL-7 $CD8^+$ T_{EFF} VLA-4 gMFI: 1910 vs 3562, p=0.0022**) and $CD8^+$ T_{SCM} cells (control IL-2 $CD8^+$ T_{SCM} VLA-4 gMFI vs control IL-7 $CD8^+$ T_{SCM} VLA-4 gMFI: 1419 vs 3271, p=0.0022**, GBM IL-2 $CD8^+$ T_{SCM} VLA-4 gMFI vs GBM IL-7 $CD8^+$ T_{SCM} VLA-4 gMFI: 1558 vs 3407, p=0.0022**).

(J) Cytotoxicity assay using progressively increasing concentrations of BRiTE co-cultured with tumor cells (U87vIII) and donor/glioblastoma hPBMCs expanded with either IL-2 or IL-7. Tumor cells were labelled with cell-trace violet after 24 hours of co-culture and analyzed via flow cytometry to assess viability. Similar cytotoxicity profiles were observed across all conditions, particularly above concentrations of 10^4 picograms/mL BRiTE.

Statistical analyses performed using two-tailed Mann-Whitney U and data presented as mean ± SEM unless specified.

Supplemental Figures

Supplemental Figure 1.

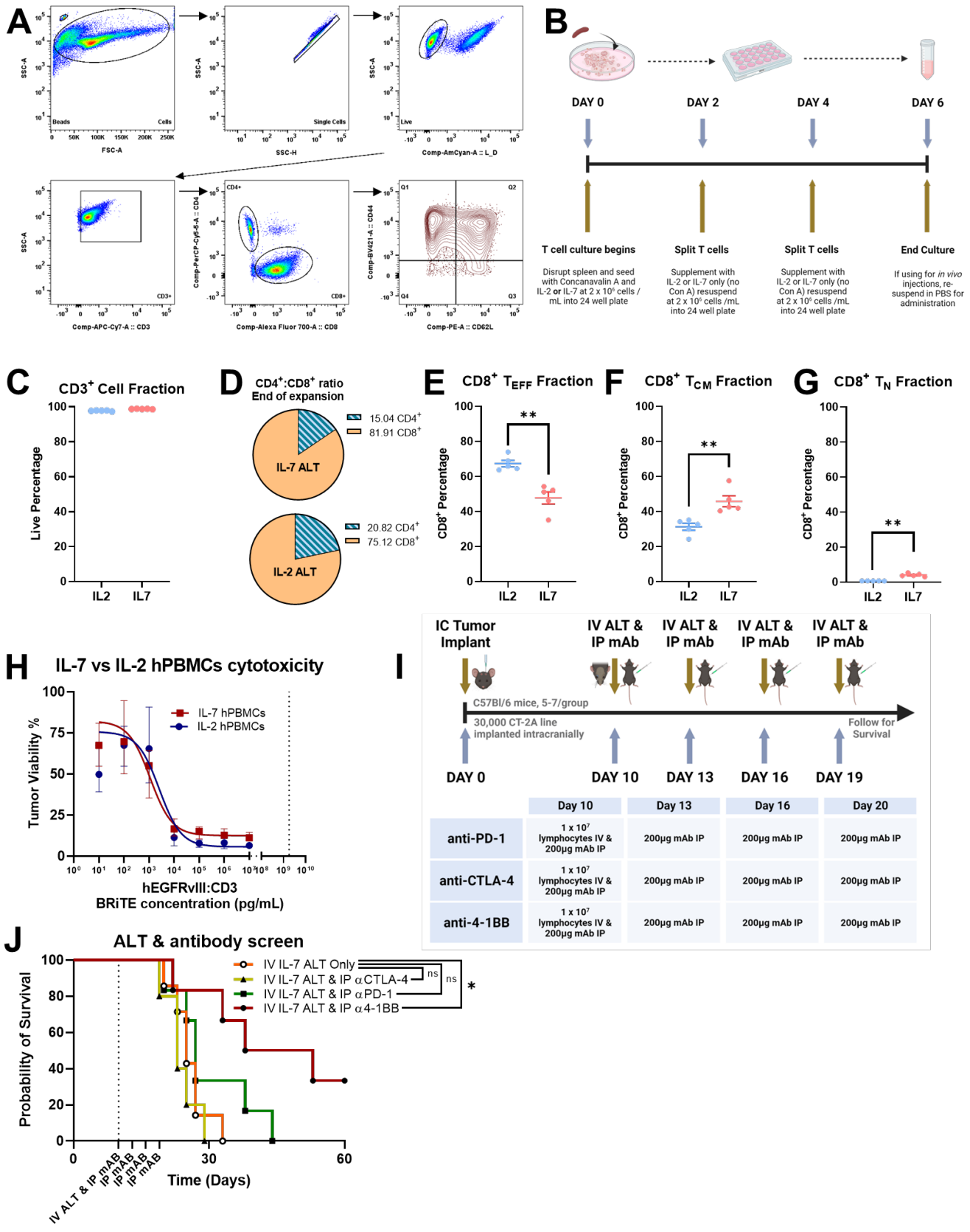

Supplemental Figure 1.

(A) Representative gating strategy shown for phenotypic analysis of cellular product at end of expansion process.

(B) Overview of *ex vivo* T cell culturing process. Spleens were harvested from C57/Bl6 mice, disrupted, and cultured in T cell media supplemented with IL-2 or IL-7 and stimmed with Concanavalin A beads before expansion over 5-7 days (n=5/group).

(C) At expansion end, >90% of cellular product consisted of $CD4^+$ & $CD8^+$ cells for both IL-2 and IL-7 expansion conditions (average fraction 97.77% for IL-2, average fraction 98.78% for IL-7, n=5/group).

(D) Both expansion conditions yielded similar skewing towards $CD8^+$ (IL-2 average $CD4^+$:$CD8^+$ 20.82%:75.12%, IL-7 $CD4^+$:$CD8^+$ 15.04%:81.91%).

(E) Expansion with IL-2 resulted in significantly increased $CD8^+$ T_{EFF} fractions compared to IL-7 (IL-2 average 65.93% vs IL-7 median 51.16%, p=0.0008***).

(F) IL-7 expansion significantly increased $CD8^+$ T_{CM} fractions compared to IL-2 (IL-7 median 42.65% vs IL-2 median 32.67%, p=0.0079**).

(G) T_N fractions were low at the end of the expansion process with both cytokines, although IL-7 maintained slightly greater naïve populations than IL-2 (IL-7 median 3.77% vs IL-2 median 0.7%, p=0.0079**).

(H) Cytotoxicity assay using progressively increasing concentrations of BRiTE co-cultured with tumor cells (U87vIII) and hPBMCs expanded with either IL-2 or IL-7. Tumor cells were labelled with cell-trace violet after 24 hours of co-culture and analyzed via flow cytometry to assess viability. Non-linear fitted dose-response curves shown with SEM (n=12/group).

(I & J) Study overview and findings of a screening approach to identify the best combinatorial mAb based approach with ALT. C57BL/6 mice (n=5-6/group) were implanted IC with 3 x 10^4 cells of syngeneic glioma (CT-2AvIII) and treated IV with 1 x 10^7 ALT on Day 10 (treatment start shown as dashed vertical line), along with 200µg of IP mAb (anti-PD-1, anti-CTLA-4 or anti-4-1BB). IP mAb Injections were given every 3 days for 4 total cycles (D10, D13, D16 & D19). Only combination ALT and anti-4-1BB produced significantly increased survival benefit compared to ALT alone (median survival 45.5 days for combination versus 25 days in ALT only group, p=0.0134*, chi-square test). Survival comparisons performed via Chi-Squared test.

Statistical analyses performed using two-tailed Mann-Whitney U and data presented as mean ± SEM unless otherwise specified. Experimental outlines generated using BioRender.com.

Supplemental Figure 2.

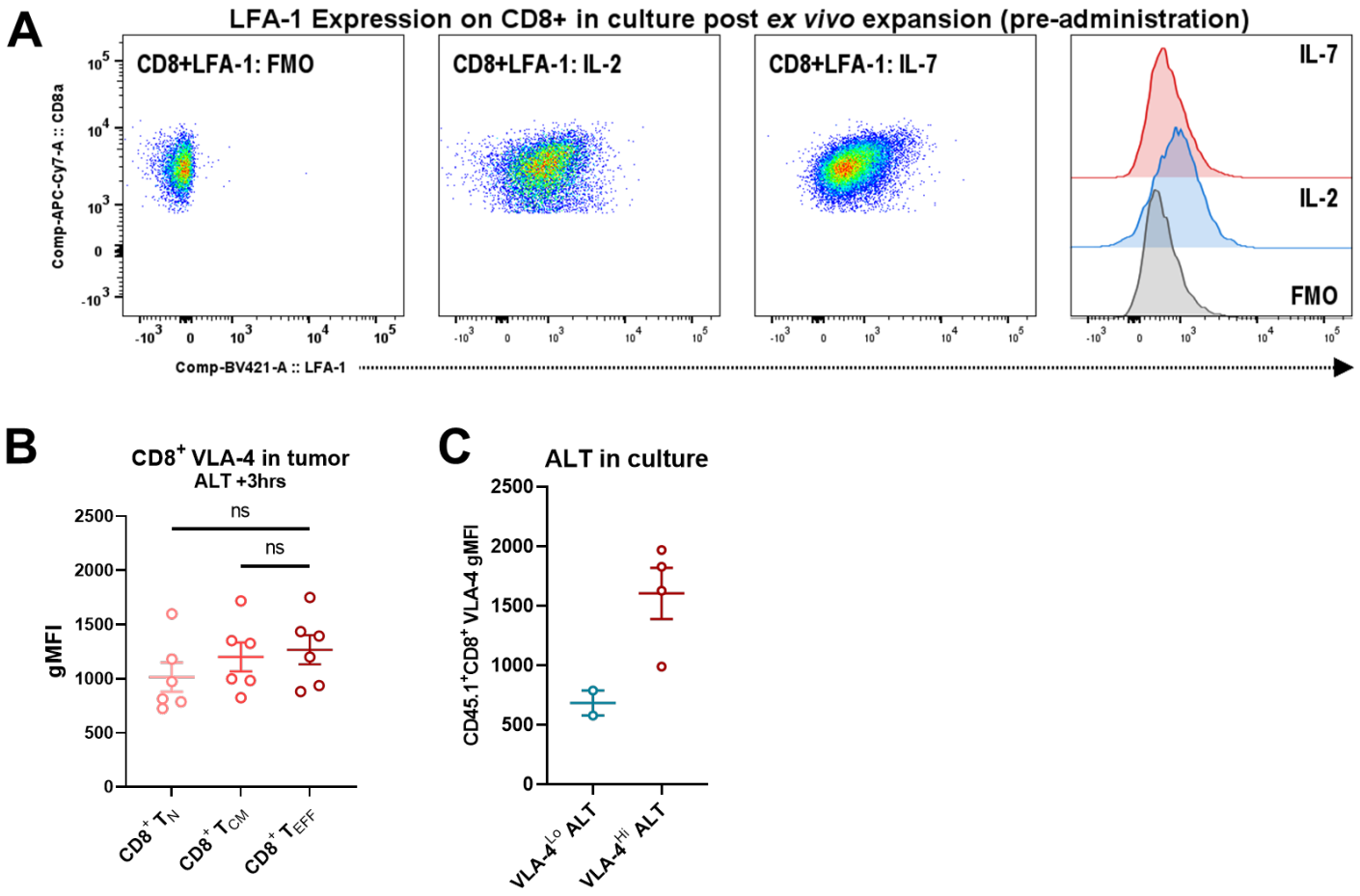

Supplemental Figure 2.

(A) Gating strategy for LFA-1 shown, no clear shift in gMFI or population was observed between IL-2 ALT or IL-7 ALT.

(B) Increased VLA-4 gMFI on tumor T cells were highest on the CD8+ T_{EFF} subset although this was not significantly increased compared to CD8+ T_{CM} or CD8+ T_N subsets (n=6/group). $CD8^+$ T_{EFF} vs T_{CM}, p=0.6991, $CD8^+$ T_{EFF} vs T_N, p=0.1797.

(C) Pooled analyses of lymphocyte expansions (representative of 3 experiments) with IL-7 that yielded VLA-4^{Hi} or IL-2 that yielded VLA-4^{Lo} (VLA-4^{Hi} geometric gMFI 1603, SD ±374.3, n=4 vs VLA-4^{Lo} mean gMFI 683, SD ±105, n=2).

Statistical analyses performed using two-tailed Mann-Whitney U and data presented as mean ± SEM unless otherwise specified.

Supplemental Figure 3.

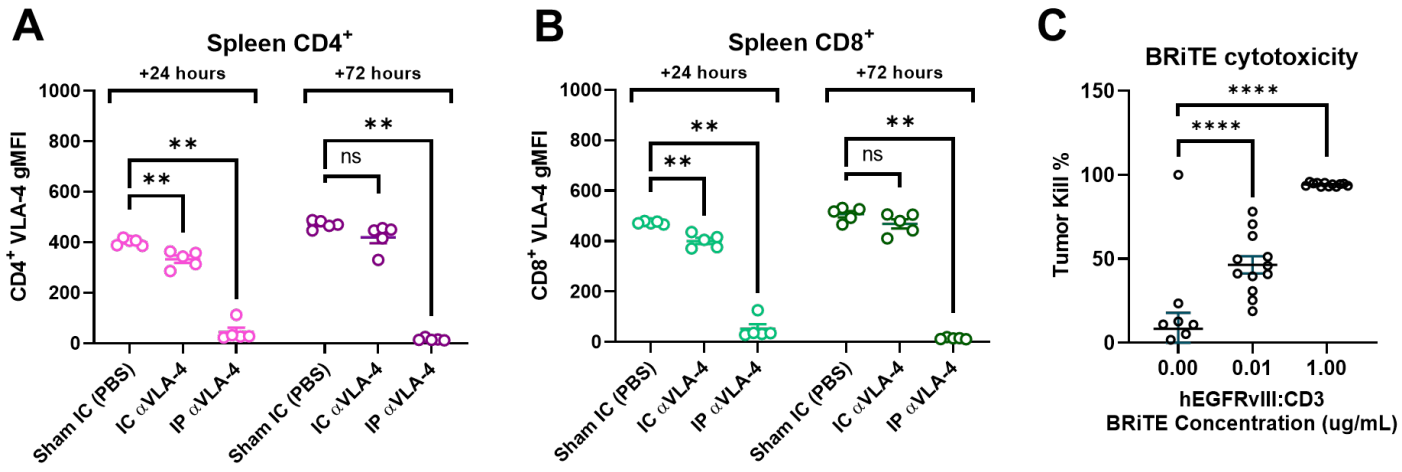

Supplemental Figure 3.

(A & B) Splenic CD4⁺ and CD8⁺ lymphocyte VLA-4 expression shown (n=5/group). VLA-4 MFI transiently dropped 24-hours following IC treatment compared to sham controls, although this returned to normal by 72-hours post administration (splenic CD4⁺ 24-hr sham IC vs IC αVLA-4, p=0.0079**; 72-hr sham IC vs IC αVLA-4, p=0.0556 and splenic CD8⁺ 24-hr sham IC vs IC αVLA-4, p=0.0079**; 72-hr sham IC vs IC αVLA-4, p=0.1508).

(C) *In vitro* cytotoxicity assay with progressively increasing BRiTE concentrations. BRiTE was co-cultured with tumor cells (U87vIII) and hPBMCs. Tumor cells were labelled with cell-trace violet after 24 hours of co-culture and analyzed via flow to assess viability. We established concentrations of BRiTE and T cells that either resulted in no kill (0.00μg/mL), 50% kill (half-maximal effective concentration, EC_{50}, 0.01μg/mL) or near total kill (1.00μg/mL).

Statistical analyses performed using two-tailed Mann-Whitney U and data presented as mean ± SEM unless otherwise specified.

Supplemental Figure 4.

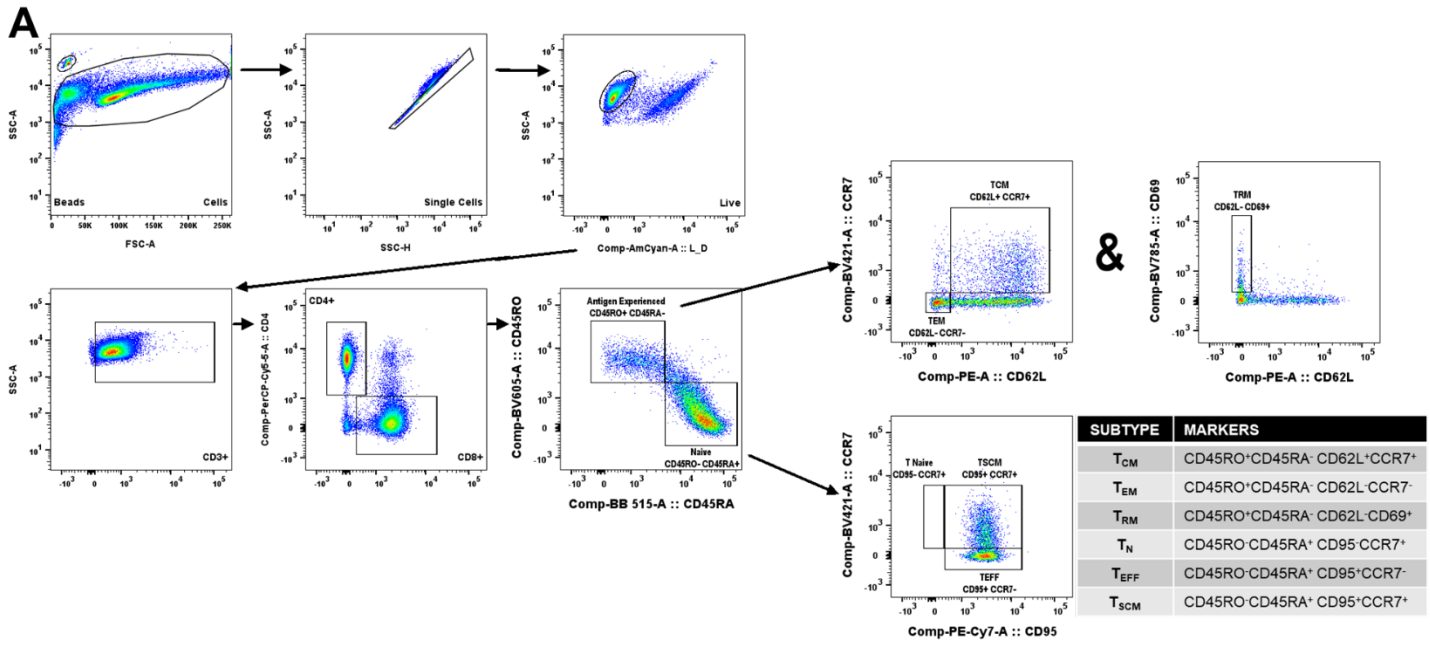

SUBTYPE	MARKERS
T_{CM}	CD45RO$^+$CD45RA$^-$ CD62L$^+$CCR7$^+$
T_{EM}	CD45RO$^+$CD45RA$^-$ CD62L$^-$CCR7$^-$
T_{RM}	CD45RO$^+$CD45RA$^-$ CD62L$^-$CD69$^+$
T_N	CD45RO$^-$CD45RA$^+$ CD95$^-$CCR7$^+$
T_{EFF}	CD45RO$^-$CD45RA$^+$ CD95$^+$CCR7$^-$
T_{SCM}	CD45RO$^-$CD45RA$^+$ CD95$^+$CCR7$^+$

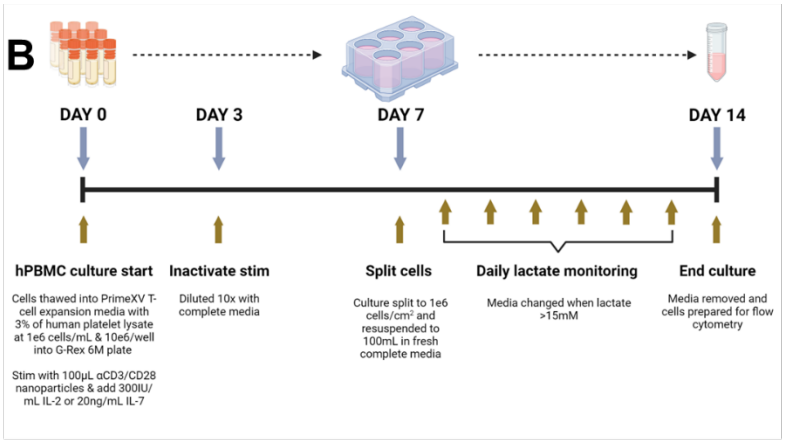

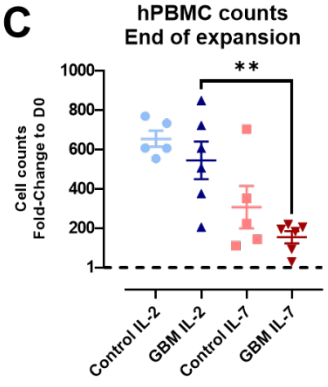

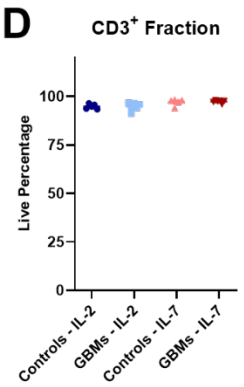

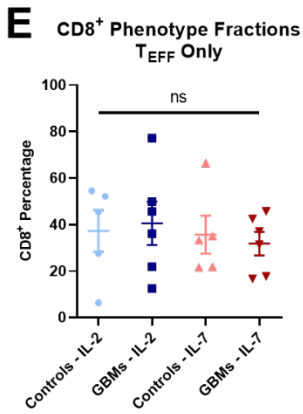

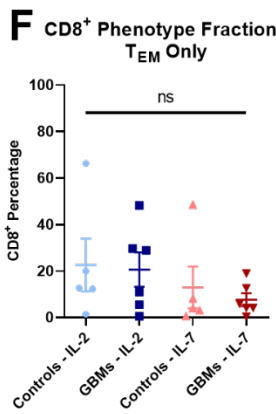

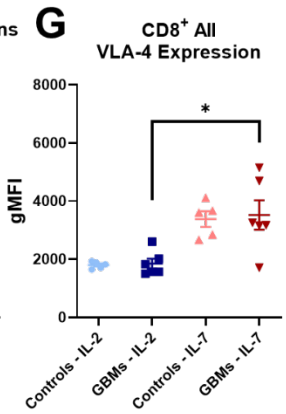

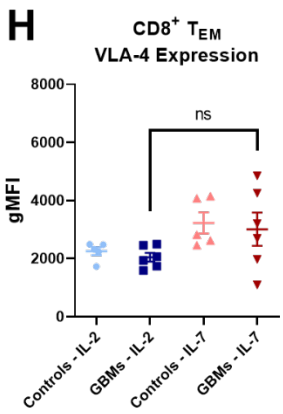

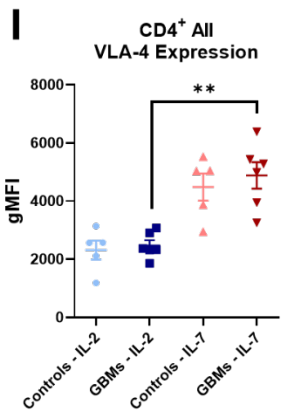

Supplemental Figure 4.

(A) Representative gating strategy shown for phenotypic analysis of cellular product at end of expansion process.

(B) Overview of *ex vivo* hPBMC culturing process. Spleens were harvested from C57/Bl6 mice, disrupted, and cultured in T cell media supplemented with IL-2 or IL-7 and stimmed with Concanavalin A beads before expansion over 5-7 days. Paired samples from control and glioblastoma groups were thawed and activated with αCD3/αCD8 nanoparticles. Cultures were maintained for 14 days in media supplemented with 300 IU/mL IL-2 as per our CAR-T expansion protocols (without transduction) or 20ng/mL IL-7. Cells were split based on lactate levels and split when lactate levels reached 15 mM (n=5-6/group).

(C) hPBMC fold-increase comparisons across all 4 groups at end of expansion. Median fold-increase for donor controls was 225.2x vs 608.7x for IL-7 vs IL-2 respectively, p=0.0556 while median fold-increase for glioblastoma patient samples was 190.3x vs 558.1x for IL-7 vs IL-2 respectively, p=0.0043**.

(D) At expansion end, cellular product consisted of ~95% $CD3^+$ across all samples and conditions.

(E & F) Sub-phenotype breakdown showed similar fractions of $CD8^+$ T_{EFF} and $CD8^+$ T_{EM} across all groups.

(G) $CD8^+$ VLA-4 mean fluorescence intensity shown across all 4 conditions. VLA-4 geometric gMFI was increased for IL-7 compared to IL-2 for both donor controls and glioblastoma samples (control IL-2 $CD8^+$ VLA-4 gMFI vs control IL-7 $CD8^+$ VLA-4 gMFI: 1804 vs 3384, p=0.0079**, GBM IL-2 $CD8^+$ VLA-4 gMFI vs GBM IL-7 $CD8^+$ VLA-4 gMFI: 1851 vs 3525, p=0.0152*).

(H) No significant difference in $CD8^+$ T_{EM} VLA-4 expression as assessed by gMFI was observed (p=0.1797).

(I) $CD4^+$ VLA-4 mean fluorescence intensity shown across all 4 conditions. VLA-4 geometric gMFI was increased for IL-7 compared to IL-2 for both donor controls and glioblastoma samples (control IL-2 $CD4^+$ VLA-4 gMFI vs control IL-7 $CD4^+$ VLA-4 gMFI: 2316 vs 4487, p=0.0159*, GBM IL-2 $CD4^+$ VLA-4 gMFI vs GBM IL-7 $CD4^+$ VLA-4 gMFI: 2477 vs 4886, p=0.0022**).

Statistical analyses performed using two-tailed Mann-Whitney U and data presented as mean ± SEM unless otherwise specified. Experimental outlines generated using BioRender.com.

Supplemental Tables

Supplemental Table 1. Overview of flow cytometry antibodies

Mouse Panel 1

Antigen	Company	Clone	Fluorophore	Catalog Number	Titrated Vol per 1e6 cells (µL)	Purpose
CD45.1	Biolegend	A20	APC	110714	1	T Cell trafficking
CD4	Biolegend	RM4-5	PerCp-Cy5.5	100540	0.5	CD4+ (Helper) T
CD8a	BD	53-6.7	APC-H7	560182	3	CD8+ (Cytotoxic) T
CD44	BD	IM7	BV786	563736	1	Memory
CD62L	BD	MEL-14	BB515	565261	0.5	Memory
VLA-4	Biolegend	R1-2	PE-Dazzle 594	103626	1	Integrin
LFA-1	BD	M18/2	BV421	744597	3	Integrin
CD45.2	BD	104	BV605	563051	3	T cell trafficking
PD-1	Biolegend	29F.1A12	PE	135205	1	Exhaustion
CD3 epsilon	Biolegend	145-2C11	BV711	100349	1	T -Cells

Mouse Panel 2

Antigen	Company	Clone	Fluorophore	Catalog Number	Titrated Vol per 1e6 cells (µL)	Purpose
CD3	Biolegend	17A2	APC-Cy7	100222	1	T-Cells
CD4	Biolegend	GK1.5	PerCP-Cy5.5	100434	3	CD4+ (Helper) T
CD8	Biolegend	53-6.7	AF700	100730	5	CD8+ (Cytotoxic) T
CD45.1	Biolegend	A20	BV785	110743	3	Exogenous
CD45.2	Biolegend	104	PE-Cy7	109830	1	Endogenous
CD44	Biolegend	IM7	BV421	103040	1	Memory
CD62L	Biolegend	MEL-14	PE	104408	3	Memory
CD69	Biolegend	H1.2F3	AF647	104518	3	Activation
CD25	Biolegend	PC61	BV711	102049	3	Activation
CD49d (VLA-4)	Biolegend	R1-2	PE-Dazzle 594	103626	3	Integrin
CD18 (LFA-1)	BD	C71/16	BV650	740465	1	Integrin

Human Panel 1

Antigen	Company	Clone	Fluorophore	Catalog Number	Titrated Vol per 1e6 cells (µL)	Purpose
CD3	BD	SK7	APC-H7	560176	3	T-Cells
CD4	Biolegend	SK3	PerCP-Cy5.5	344608	1	CD4+ (Helper) T
CD8	Biolegend	SK1	AF700	344724	1	CD8+ (Cytotoxic) T
CD45RA	BD	HI100	BB515	564552	0.5	Memory
CD45RO	Biolegend	UCHL1	BV605	304238	3	Memory
CD62L	Biolegend	DREG-56	PE	304806	1	Memory
CCR7	Biolegend	G043H7	BV421	353208	5	Memory
CD95	Biolegend	DX2	PE-Cy7	305622	1	Fas
CD69	Biolegend	FN50	BV785	310932	3	Early Activation
HLA-DR	Biolegend	L243	APC	307610	5	Activation
CD49d (VLA-4)	Biolegend	9F10	PE-Dazzle 594	304326	1	Integrin
CD18 (LFA-1)	BD	L130	BV650	744553	5	Integrin

Viability assessed across panels using LIVE/DEAD™ Fixable Aqua Dead Cell Stain Kit, ThermoFisher, Catalog Number #L34966